

**EFFECTS OF MASONRY INFILL WALLS ON THE SEISMIC
PERFORMANCE OF BUILDINGS**

MEHMET SELİM ÖZTÜRK

DECEMBER 2005

**EFFECTS OF MASONRY INFILL WALLS ON THE SEISMIC
PERFORMANCE OF BUILDINGS**

**A THESIS SUBMITTED TO
THE GRADUATE SCHOOL OF NATURAL AND APPLIED SCIENCES
OF
MIDDLE EAST TECHNICAL UNIVERSITY**

BY

MEHMET SELİM ÖZTÜRK

**IN PARTIAL FULFILLMENT OF THE REQUIREMENTS
FOR
THE DEGREE OF MASTER OF SCIENCE
IN
CIVIL ENGINEERING**

DECEMBER 2005

Approval of the Graduate School of Natural and Applied Sciences

Prof. Dr. Canan Özgen
Director

I certify that this thesis satisfies all the requirements as a thesis for the degree of Master of Science.

Prof. Dr. Erdal Çokça
Head of Department

This is to certify that we have read this thesis and that in our opinion it is fully adequate, in scope and quality, as a thesis for the degree of Master of Science.

Assoc. Prof. Dr. Ahmet Yakut
Co-Supervisor

Assoc. Prof. Dr. Uğurhan Akyüz
Supervisor

Examining Committee Members

Assoc. Prof. Dr. Cem Topkaya (METU, CE)

Assoc. Prof. Dr. Uğurhan Akyüz (METU, CE)

Assoc. Prof. Dr. Ahmet Yakut (METU, CE)

Asst. Prof. Dr. Barış Binici (METU, CE)

M.S. Volkan Aydoğan (PROYA YAZILIM)

I hereby declare that all information in this document has been obtained and presented in accordance with academic rules and ethical conduct. I also declare that, as required by these rules and conduct, I have fully cited and referenced all material and results that are not original to this work.

Name, Last name : Mehmet Selim ÖZTÜRK

Signature :

ABSTRACT

EFFECT OF MASONRY INFILL WALLS ON THE SEISMIC PERFORMANCE OF BUILDINGS

ÖZTÜRK Mehmet Selim

M. Sc., Department of Civil Engineering

Supervisor: Assoc. Prof. Dr. Uğurhan AKYÜZ

Co-Supervisor: Assoc. Prof. Dr. Ahmet YAKUT

December 2005, 88 pages

In Turkey, in most of the reinforced concrete buildings, hollow masonry infill walls are used as non-structural partition walls. Since they are used as a non-structural member, during design stage, their contribution to overall building behavior is not well known. Observations made after the earthquakes revealed that these non-structural elements had beneficial effects on the lateral capacity of the building.

In this study, the contribution of the hollow masonry infill walls to the lateral behavior of reinforced concrete buildings was investigated. For this purpose, two different buildings were chosen as case studies. Three and six story symmetric buildings are modeled as bare and infilled frames. The parameters that were investigated are column area, infill wall area, distribution of masonry infill walls

throughout the story. To determine the effect of each parameter, global drift ratios are computed and are compared for each case.

Keywords: Earthquake, masonry infill wall, column area, infill wall area

ÖZ

TUĞLA DOLGU DUVARLARIN BİNALARIN SİSMİK DAVRANIŞI ÜZERİNE ETKİLERİ

ÖZTÜRK Mehmet Selim

Yüksek Lisans, İnşaat Mühendisliği Bölümü

Tez Yöneticisi: Doç. Dr. Uğurhan AKYÜZ

Ortak Tez Yöneticisi: Doç.Dr. Ahmet YAKUT

Aralık 2005, 88 pages

Türkiye'deki betonarme binaların çoğunda, boşluklu tuğlalı dolgu duvarlar yapısal olmayan bölme duvar olarak kullanılmaktadır. Yapısal olmayan eleman olarak kullanıldıkları için, dolgu duvarların bina davranışına yaptıkları katkı tasarım aşamasında iyi bilinmemektedir. Depremlerden sonra yapılan incelemeler, yapısal olmayan elemanların binanın yanal kapasitesine yararlı yönde etki ettiklerini ortaya çıkarmıştır.

Bu çalışmada, boşluklu tuğlalı dolgu duvarların betonarme binaların yanal davranışına katkısı incelenmiştir. Bu amaçla, iki farklı bina durum çalışması olarak seçilmiştir. Üç katlı simetrik ve altı katlı simetrik olan bu iki bina çıplak ve dolgu duvarlı olarak modellenmiştir. Kolon alanı, dolgu duvar alanı ve dolgu duvarların kat içinde dağılımı incelenen parametrelerdir. Her bir parametrenin

etkisini anlamak için binaların yanal ötelenme oranları hesaplanmış ve birbirleri ile mukayese edilmiştir.

Anahtar Kelimeler: Deprem, tuğla dolgu duvar, kolon alanı, dolgu duvar alanı

Dedicated to my family

ACKNOWLEDGEMENTS

I would like to express my deepest gratitude to my supervisor Assoc. Prof. Dr. Uğurhan Akyüz and co-supervisor Assoc. Prof. Dr. Ahmet Yakut for their support and encouragement during this study.

I also would like to thank Prof. Dr. Güney Özcebe for his invaluable suggestion and guidance since the first year of my undergraduate education.

Special thanks go to my friends Kübra Berke and Burak Keser for their great motivations throughout the study.

I would like to extend my thanks to Barış Yalım, Melih Süsoy, Bayezid Özden for their priceless support and friendship during the entire study.

Finally, I would like to present my deepest thanks to my family for their endless love, support and encouragements throughout all my life.

TABLE OF CONTENTS

	PAGE
PLAGIARISM.....	iii
ABSTRACT.....	iv
ÖZ.....	vi
DEDICATION.....	viii
ACKNOWLEDGEMENTS.....	ix
TABLE OF CONTENTS.....	x
LIST OF TABLES.....	xiii
LIST OF FIGURES.....	xvi
CHAPTER	
1. INTRODUCTION	1
1.1 GENERAL.....	1
1.2 LITERATURE SURVEY.....	3
1.3 OBJECTIVE AND SCOPE	5

2.	ANALYSIS OF R/C FRAMES WITH INFILL WALLS.....	7
2.1	INTRODUCTION.....	7
2.2	DETERMINATION OF EQUIVALENT STRUT WIDTH.....	9
2.2.1	SMITH & CARTER METHOD [6]	9
2.2.2	FEMA 273 METHOD [7].....	14
2.3	FAILURE MODES OF MASONRY INFILLED R/C FRAMES	15
3.	DESCRIPTION AND ANALYSIS OF CASE STUDY	
	BUILDINGS.....	19
3.1	INTRODUCTION.....	19
3.2	DESCRIPTION OF CASE STUDY BUILDINGS.....	20
3.2.1	CASE I – THREE STORY BUILDING.....	20
3.2.2	CASE II – SIX STORY BUILDING.....	23
3.3	ANALYSIS OF BUILDINGS	26
3.3.1	MODELLING ASSUMPTIONS.....	26
3.3.2	LINEAR ANALYSIS PROCEDURE.....	28
3.3.2.1	CASE I.....	29
3.3.2.2	CASE II	31
3.3.3	PARAMETRS CONSIDERED AND THEIR RANGES.	33
3.3.3.1	COLUMN SIZE.....	35
3.3.3.2	INFILL WALL AREA.....	37
3.3.3.3	ARRAGEMENT OF INFILL WALL.....	38
3.3.3.3.1	CASE I	39
3.3.3.3.2	CASE II	44

3.3.4	RESULTS OF SAMPLE ANALYSIS	49
3.3.5	SUMMARY OF ANALYSES.....	51
4.	INTERPRETATION AND DISCUSSION OF RESULTS.....	55
4.1	INTRODUCTION.....	55
4.2	EFFECT OF COLUMN SIZE.....	56
4.3	EFFECT OF INFILL WALL THICKNESS.....	64
4.4	RECOMMENDED RELATION FOR GIVEN GLOBAL DRIFT RATIO.....	71
4.5	EFFECT OF INFILL WALL ARRANGEMENT	77
5.	CONCLUSIONS AND RECOMMENDATIONS.....	83
5.1	INTRODUCTION.....	83
5.2	CONCLUSIONS.....	84
5.3	RECOMMENDATIONS.....	85
	REFERENCES.....	86

LIST OF TABLES

TABLE		PAGE
3.1	Compression Strut Properties for Case I (Initial Model).....	20
3.2	Compression Strut Properties of Case II (Initial Model).....	23
3.3	Concrete Material Properties.....	26
3.4	Dead Load Component for One Story for Case I.....	29
3.5	Story Weights for Case I.....	30
3.6	Seismic Load Acting on Each Story (Case I).....	31
3.7	Dead Load Component for One Story for Case II.....	31
3.8	Story Weights for Case II.....	32
3.9	Seismic Load Acting on Each Story (Case II).....	32
3.10	Compression Strut Widths for Different Column Sizes (Case I).....	36
3.11	Compression Strut Widths for Different Column Sizes (Case II).....	37
3.12	Compression Strut Widths (Case I).....	38
3.13	Compression Strut Widths (Case II).....	38
3.14	a) Wall Properties in X-direction (Case I).....	43
	b) Wall Properties in Y-direction (Case I).....	43
3.15	a) Wall Properties in X-direction (Case II).....	48

	b) Wall Properties in Y-direction (Case II)	48
3.16	Inter-Story Drift Ratio for Sample Analysis	49
3.17	a) Shear Contribution of Elements in X-Direction.....	50
	b) Shear Contribution of Elements in Y-Direction.....	50
3.18	Identification of Buildings.....	52
4.1	Global Drift Ratios for Case I	57
4.2	Global Drift Ratios for Case II.....	57
4.3	Percentage Reduction in Global Drift Ratio for Case I.....	61
4.4	Percentage Reduction in Global Drift Ratio for Case II.....	62
4.5	Wall Index for Different Wall Thicknesses.....	65
4.6	Global Drift Ratio for Case I.....	65
4.7	Global Drift Ratio for Case II.....	65
4.8	Percentage Reduction in Global Drift Ratio for Different <i>CI</i>	69
4.9	Target Global Drift Ratios.....	71
4.10	Wall-Column Relation for $\Delta_{max} / H = 0.003$ (Case I)	72
4.11	Wall-Column Relation for $\Delta_{max} / H = 0.005$ (Case I)	72
4.12	Wall-Column Relation for $\Delta_{max} / H = 0.01$ (Case I)	73
4.13	Wall-Column Relation for $\Delta_{max} / H = 0.006$ (Case II).....	74
4.14	Wall-Column Relation for $\Delta_{max} / H = 0.010$ (Case II)	75
4.15	Wall-Column Relation for $\Delta_{max} / H = 0.0150$ (Case II)	75
4.16	a) Comparison of Results for <i>FE</i> (Case I).....	78

	b) Comparison of Results for <i>SM</i> (Case I).....	79
4.17	a) Comparison of Results for <i>FE</i> (Case II).....	80
	b) Comparison of Results for <i>SM</i> (Case II).....	81

LIST OF FIGURES

FIGURE	PAGE
2.1 a) Laterally Loaded Infilled Frame [6].....	8
b) Equivalent Frame [6].....	8
2.2 Length of Contact, α	11
2.3 Equivalent Strut Widths as a Function of λh [6].....	13
2.4 Failure Modes of Reinforced Concrete Frames [5].....	16
2.5 Failure Modes of Infill [5].....	16
2.6 Sliding Shear Failure of Infill [4].....	18
3.1 Typical Floor Plan for Case I.....	21
3.2 Frame in X- and Y- Directions for Case I.....	22
3.3 Typical Floor Plan for Case II.....	24
3.4 Frame in X- and Y- Directions for Case I.....	25
3.5 Compression Strut Connection.....	27
3.6 a) Wall Arrangements of Model I for Case I	40
b) Wall Arrangements of Model II for Case I.....	41
c) Wall Arrangements of Model III for Case I.....	42

3.7	a) Wall Arrangements of Model I for Case II.....	45
	b) Wall Arrangements of Model II for Case II.....	46
	c) Wall Arrangements of Model III for Case III.....	47
4.1	a) Drift Ratio in X-dir. vs. CI_x for Case I	58
	b) Drift Ratio in Y-dir. vs. CI_y for Case I.....	58
4.2	a) Drift Ratio in X-dir. vs. CI_x for Case II.....	60
	b) Drift Ratio in Y-dir. vs. CI_y for Case II.....	60
4.3	% Reduction in Global Drift Ratio for Different WI	63
4.4	a) Drift Ratio in X-dir. vs. WI_x for Case I.....	66
	b) Drift Ratio in Y-dir. vs. WI_y for Case I.....	66
4.5	a) Drift Ratio in X-dir. vs. WI_x for Case II.....	67
	b) Drift Ratio in Y-dir. vs. WI_y for Case II.....	68
4.6	% Reduction in Global Drift Ratio for Different CI	70
4.7	Graph of Column Ratio versus Wall Ratio (Case I).....	73
4.8	Graph of Column Ratio versus Wall Ratio (Case II).....	76
4.9	Column and Wall Ratios Required to Limit MGSD	77

CHAPTER 1

INTRODUCTION

1.1 GENERAL

In Turkey, hollow masonry infilled reinforced concrete frame is one of the most common structural system. The simplicity of construction and highly developed expertise have made the infilled frame one of the most rapid and economical structural form for reinforced concrete buildings. Hollow masonry infills are functioning mostly as partitions and exterior walls, and rarely as walls around stairs, elevator, and service shafts.

There are two different approaches for designing masonry infilled concrete frames depending on local construction site. In the first approach, masonry infill is taken as a part of structural system and they are assumed to brace the frame against horizontal loading. In the second approach, the frame is designed to carry the total vertical and horizontal loading. Moreover, masonry infill is uncoupled to avoid load being transferred to them. In earthquake prone regions like Turkey, hollow masonry infill walls are counted as non-structural elements. They are not taken into account at design stage. Although they are intended to be uncoupled from the load carrying system, frequently observed diagonal cracking on masonry infill walls also show that the approach is not always valid. Masonry infill walls sometimes affect the mode of behavior significantly. As known, masonry is a very brittle material. To absorb huge amount of energy originated by seismic action

with high intensity, the structure needs ductility. In case of well designed frames, presence of very stiff but brittle masonry walls may reduce the ductility level of whole system. However, flexible frame with stiff masonry infill results in a relative stiff and tough bracing system in case of earthquake with low or moderate intensity. In addition to that, the natural period of the structural system may be shortened. This situation results in a different input level to the system. Also, sharing of story shear between frames in the same direction may be changed according to presence of masonry infill. And some columns may sustain more force than that assumed in the original design. This means that distribution of masonry infill gains importance on behavior. Some system deficiencies are also caused by masonry infill walls. Improper arrangement of partition walls or some architectural necessities cause asymmetry, short column, weak story or soft story problems. The earthquakes occurred in August 1999 and November 1999 (Kocaeli and Düzce Earthquakes) showed that one of the main reasons of tremendous destruction is due to the deficiencies. Although improper distribution of masonry infill wall may create some lateral deficiencies, investigations after major earthquakes in Turkey showed that the presence of these non-structural walls help to the building and increase the lateral capacity up to a certain limit. Surveys on lightly and moderately damaged buildings after major earthquakes showed that damage level of some buildings is less than the anticipated level. This result was attributed to the presence of infill walls and their contribution to lateral strength of whole system.

Turkish Seismic Code (ABYYHY 98) [1] has provisions to minimize irregularities and deficiencies caused by infill walls. However, infill walls are considered as secondary or non-structural elements. These non-structural elements are not taken into account in the design. This means that the contribution of the infill walls to lateral stiffness and lateral strength of the whole system is neglected. This study aims to investigate their effect on the seismic performance of the buildings.

1.2 LITERATURE SURVEY

Past relevant studies on masonry and masonry infilled concrete frames and their lateral performance are presented in this part.

Sucuoğlu & McNiven [2] studied seismic response of reinforced masonry piers that reveal a shear mode of failure. Their study consisted of two parts: first, the results of an experimental program on reinforced masonry piers under cyclic lateral loads were presented. Then some seismic code provisions about seismic design of masonry were evaluated under the light of the experimental observations. They focused on the seismic shear response of reinforced masonry piers. Shear is the dominant failure mode due to the low aspect ratios and high gravity load imposed on piers. They proposed a shear design concept for masonry piers based on experimental observations and analytical evaluation of masonry behavior at ultimate shear resistance level. Their design method was based on diagonal cracking strength of masonry piers. Also web reinforcement was used in design method to provide post cracking capacity. They concluded that vertical loads have strong effect on both cracking and ultimate strength level. Moreover, the results of the proposed method, which determined the design shear and the amount of web reinforcement essential for ductile resistance, matched with the experimental results.

Sucuoğlu & Erberik [3] studied seismic performance of a three-story unreinforced masonry building which survived in 1992 Erzincan earthquake without damage. First, a set of experiments were performed to determine the mechanical properties of the masonry walls. Then an accurate model was developed for the non-linear dynamic analysis of masonry building with the help of a computer program. Results of performed dynamic analysis, namely the modal spectrum analysis, incremental collapse analysis and time-history analysis, showed that if it satisfies the requirement of seismic code, unreinforced masonry buildings have considerable lateral load resistance both in elastic and ultimate limit state. They showed that masonry wall elements have remarkable energy dissipation capacity

because of internal friction. (However, these entire conclusions were based on the mechanical properties that were obtained by laboratory tests. In other words, validity of these conclusions is dependent on achievement of the same material properties.)

Paulay & Priestley [4] proposed a theory about the seismic behavior of masonry infilled frame and a design method for infilled frames. Authors said that although masonry infill may increase the overall lateral load capacity, it can result in altering structural response and attracting forces to different or undesired part of structure with asymmetric arrangement. This means that masonry infill may cause structural deficiencies. In [4], infilled frames behave differently with respect to lateral load level. At low levels, both concrete frame and infill act in a fully composite manner.

Smith & Coull [5] presented a design method for infilled frame based on diagonally braced frame criteria. The developed method considered three possible modes of failure of infill: shear along the masonry, diagonal cracking through masonry and crushing of a corner of infill. They assumed effective width of diagonal compression strut as equal to one-tenth of the diagonal length of the infill panel. At the initial design stage, frame must be designed on the basis of the gravity loading.

Smith & Carter [6] examined multi-story infilled frames for the case of lateral loading. In the light of experimental results, authors proposed design graphs and design method based on an equivalent strut concept. First, they focused on the composite behavior of infilled frame and failure modes. Then, the factors that affect the effective width of diagonal compression strut were determined. Finally, with known factors and behavior, the design curves to estimate equivalent strut width, cracking and crushing strength of infill panel were presented.

Federal Emergency Management Agency (FEMA) prepared FEMA 273 [7], the *NEHRP Guidelines for the Seismic Rehabilitation of Buildings*, to guide design

professionals, for the seismic rehabilitation of buildings. Design professionals can use this document for design and analysis of seismic rehabilitation project. However, this document is not a code. In this document, analysis procedures, material properties and design criteria for concrete, steel, masonry and light weight materials are given in separate chapters. In the chapter devoted to concrete, there are general provisions about infilled concrete frames. According to these provisions, concrete frames with infill walls must be constructed in such a way that the infill and frame interact when subjected to design loads. Material properties, young's modulus and stiffness parameter of masonry which is used as infill are explained in detail.

1.3 OBJECTIVE AND SCOPE

The main objective of this study is to investigate the contribution of hollow masonry infill walls to lateral strength and lateral stiffness of the buildings. A comparative study was performed on 3-D analysis model created in ETABS [8], a commercial computer program for the analysis of structures. Hollow masonry infill walls were modeled as compression struts. Their tensile capacities, which were negligible, were disregarded. While modeling the hollow masonry infill walls as compression struts, two different approaches were considered: namely Smith and Carter method [6] and FEMA 273 Method [7]. In order to compare and understand the effect of hollow masonry infill walls, analyses were also carried out for bare frames, i.e. without any non-structural infill wall. The parameters studied within the context of this thesis are:

- Infilled wall area
- Column area
- Distribution of masonry infill walls throughout the story.

To determine the effect of each parameter, global drift ratios computed in each case were compared.

In Chapter 2, theoretical basis of modeling of infilled frames is given. Equivalent strut model of infilled frame and failure modes of them are discussed. In Chapter 3, the analysis procedure followed throughout this study is explained. Information about the modeling procedure, assignment and assumptions are also given in the third chapter. Description of case study buildings and the parameters considered are also given. The third chapter ends with the presentation of results of sample analysis. In Chapter 4, the results of analysis are given in detail. Effect of masonry infill wall area, effect of column size and their relative effect on seismic behavior are investigated through the analysis of two case studies. Also the comparisons of results of each phase of each case are presented in both graphical and tabular form. Finally, the summary and main conclusions of the study together with future recommendations are provided in Chapter 5.

CHAPTER 2

ANALYSIS OF R/C FRAMES WITH INFILL WALLS

2.1 INTRODUCTION

In this chapter, behavior of masonry infilled concrete frames under the lateral load is studied. Investigations showed that, one of the most appropriate ways of analyzing the masonry infilled concrete frames is to use the diagonally braced frame analogy. Although there are many assumptions about equivalent strut properties, two of the proposed methods which define the equivalent compression strut properties are discussed in detail. These are Smith & Carter [6] method, and the method which is a part of FEMA 273 [7] guideline for seismic design. All analysis models including masonry infill wall are prepared with the guidance of these noteworthy studies.

The structure, which consists of frame and infill, is subjected to lateral loading. There is no special connection or any anchorage between frame and infill. Because of this reason, the infill and frame may be separated over a large part of side length. Only the corners of compression diagonal remain integral. This situation may be represented with equivalent strut replacing the infill. Infilled frame and the equivalent frame are shown in Figure 2.1 [6]

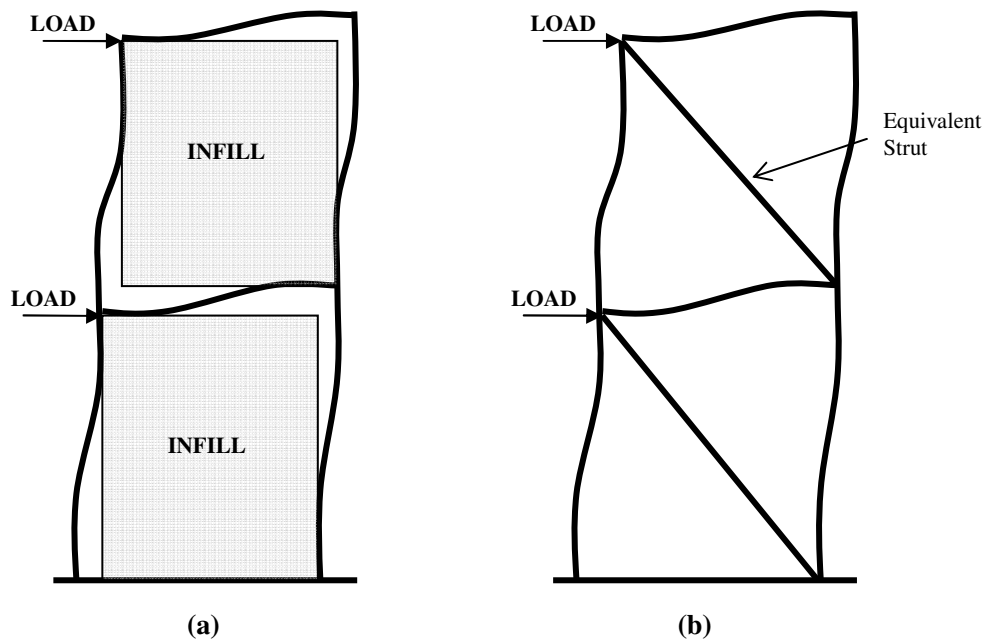


Figure 2.1(a) - Laterally Loaded Infilled Frame; **(b)** - Equivalent Frame (taken from [6])

Smith & Carter [6] examined the behavior of multi-story infilled frame under lateral loading. The main objective of their study was to obtain reasonable information about stiffness and strength of horizontally loaded infilled frames, because there was an inadequacy of information about the composite stiffness and strength of infilled system. Authors tried to develop a design method based on an equivalent strut concept. They performed a number of experiments and obtained design curves reflecting the behavior of infilled system under the action of lateral loading.

FEMA 273 [7] suggests two different approaches depending on behavior of concrete frame with masonry infill. If it can be proved that both frame and masonry infill will remain uncracked under the action of lateral loading, the analysis method can be based on linear elastic behavior and the structure can be assumed to be a homogeneous medium for stiffness computation. In other words, the frame with infill may be included to the load carrying system as a huge unique

element. On the other hand, if the frame is unable to remain uncracked, behavior of cracked concrete frame with masonry infill may be represented by diagonally braced frame. In this analogous model, columns act as vertical chords, beams act as horizontal ties and the masonry infill is modeled as an equivalent compression strut.

Before describing the procedure for determining the equivalent strut width, the material properties of the masonry must be clarified, because these are used as the basis for strength and stiffness attributes of masonry walls and infill panels. There is more than one method described in FEMA 273 [7] to determine the material properties of masonry. Instead of the described test methods, default material properties can be assigned to the masonry according to its condition: compressive strength, f_{me} , shall be taken not to exceed 6 MPa for masonry in good condition, 4 MPa for masonry in fair condition and 2 MPa for masonry in poor condition. Moreover, the prism tests showed that value for modulus of elasticity of masonry in compression, E_{me} , shall be taken as 550 times the expected compressive strength of masonry [7].

2.2 DETERMINATION OF EQUIVALENT STRUT WIDTH

2.2.1 SMITH & CARTER'S METHOD [6]

Determination of equivalent strut width gives a chance to estimate the behavior of infilled frame. With known value of equivalent width, the strength and the stiffness of frame with infill wall may be included in the lateral load resistance of the structure.

More than one parameter affects the equivalent strut width. First one is geometric properties of infill. Panel proportion and panel height are important parameters. The failure mode changes according to surrounding frame stiffness in addition to separate properties, relative properties of frame and infill take important role on

equivalent strut width. Furthermore, diagonal stiffness and strength of an infill panel directly depend on its contact length with surrounding frame. The contact length, α , can be related with the relative stiffness of the infill to frame. The approximate equation is given below,

$$\frac{\alpha}{h_{col}} = \frac{\pi}{2\lambda h_{col}} \quad (2.1)$$

where;

h_{col} : Height of the column

α : Contact length

In Equation 2.1, λh_{col} is a non-dimensional parameter expressing the relative stiffness of the frame to the infill. λ is an empirical parameter and given as;

$$\lambda = \sqrt[4]{\frac{E_{inf} \cdot t_{inf} \cdot \sin(2\theta)}{4 \cdot E_{col} \cdot I_{col} \cdot h_{inf}}} \quad (2.2)$$

where;

E_{inf} : Young's modulus of elasticity of infill

t_{inf} : Thickness of infill panel

h_{inf} : Height of infill panel

E_{col} : Young's modulus of the column

I_{col} : Moment of inertia of the column

θ : Slope of the infill diagonal to the horizontal

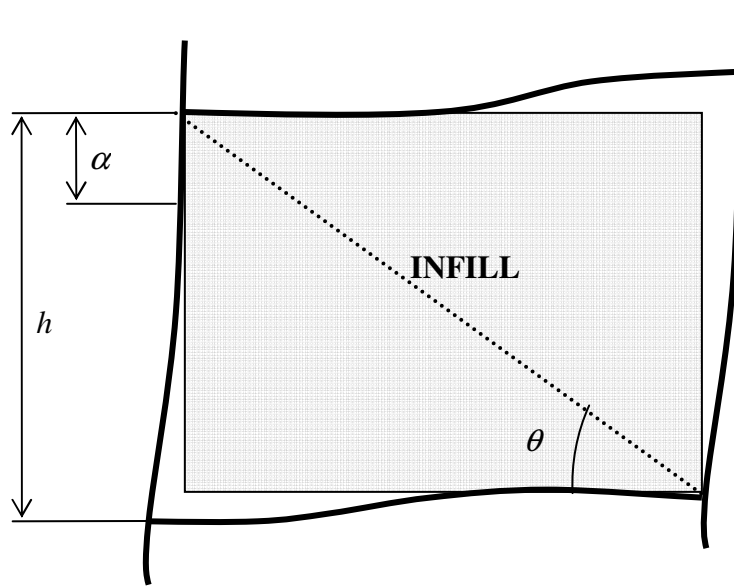


Figure 2.2 - Length of Contact, α (taken from [6])

As it can be seen from Equation 2.2, instead of all frame stiffness (beam and column) this empirical parameter is related with only the column stiffness. Experiments show that variation in beam stiffness has negligible effect on the behavior of the structure. Whatever the beam stiffness is, beam contact length is always approximately half of its span.

Modulus of Elasticity of concrete and masonry is not constant but decreases with increasing stress. Thus, the diagonal stiffness of the infill is reduced significantly. When the infilled frame is pushed in horizontal direction, a significant variation in the stress takes place along the compression diagonal. Stresses at corner are extremely higher than those at the center in the compression diagonal strut. To determine the equivalent strut width, the strains must be computed using the appropriate value of the tangent modulus of elasticity for a particular stress. Further tests on multi-story infilled frame also show that, loading level is one of the important parameters which controls the behavior of the infilled frame

structure. The resulting effective width is not a constant value for a particular infill but decrease as the loading is increased. At the beginning stage, the strut width is obtained from assuming that the infill material is of constant modulus equal to initial modulus. As the load is increased, the stresses in the infill also increase. The critical load level is reached when the stress at the loading corner is equal to the ultimate compressive strength of the infill material. Beyond that level, any increase in load causes decrease in capacity. At yielding stage, the effective strut width may be determined by assuming the strain in the loading corner to be equal to the compressive failure strain. Also the diagonal strain diagram along whole strut length requires modification. By using the compressive strength of the infill material and the known load level that causes yielding of loading corner, an approximate relationship can be determined as a function of non-dimensional parameter, λh . Using this relationship, the effective strut width can be determined for any load level that is expressed as a proportion of the ultimate strength of the infill panel. In Figure 2.3, The design charts, curve for w/d , (where d is the diagonal length), as a function of non-dimensional parameter, λh , are given for different panel proportions [6]. For each panel proportion, design curves are separately sketched four different loading conditions. i.e. $R/R_c = 0$, $R/R_c = 1/2$, $R/R_y = 1$ and $R/R_c = 1$. Where; R , R_c and R_y represent applied load, the load causing crushing of infill panel and the load causing yielding of infill panel respectively.

In analysis phases, infill walls can be represented as a strut, with determined value of w , of the same material and the thickness as the infill.

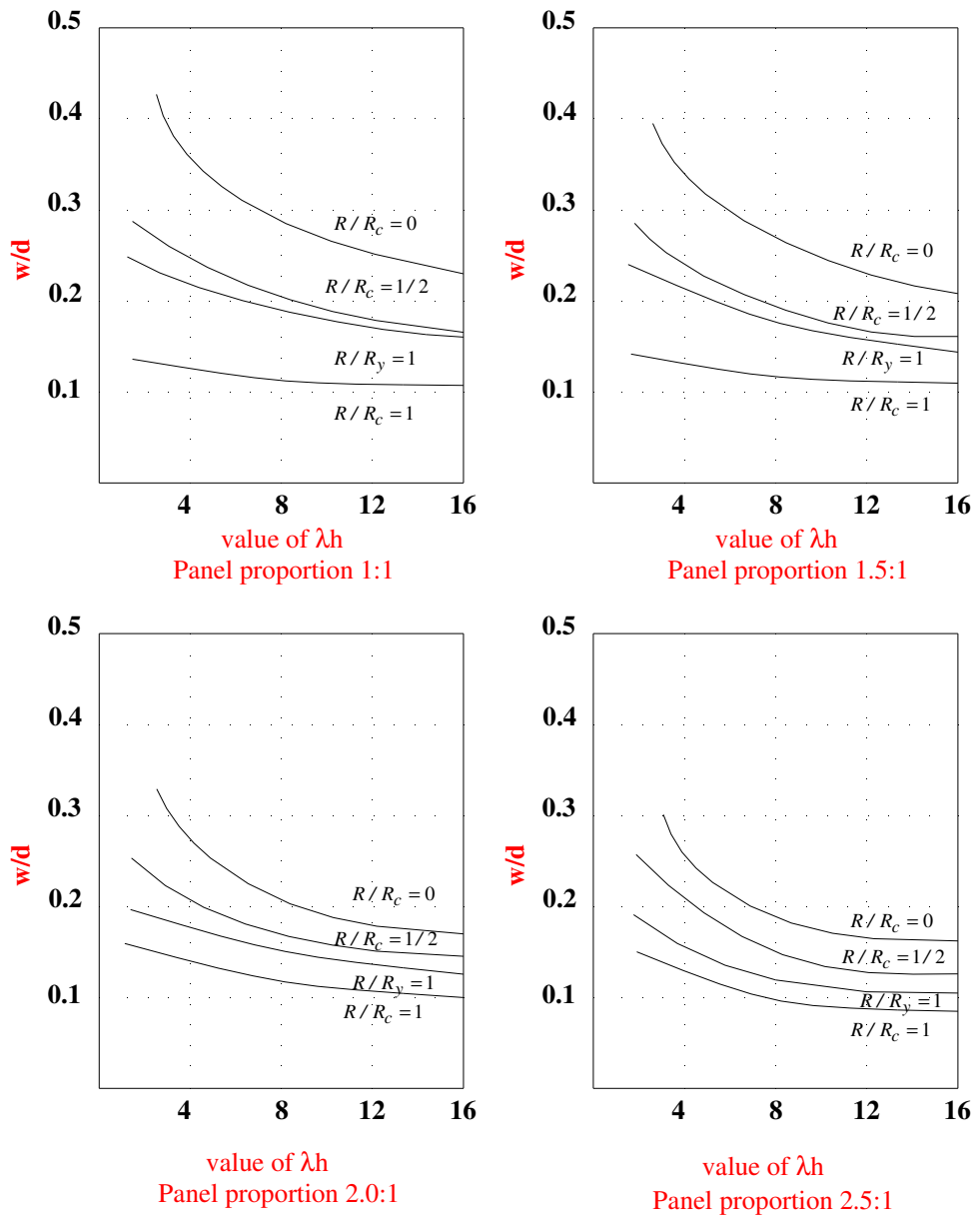


Figure 2.3 - Equivalent strut widths versus λh (taken from [6])

2.2.2 FEMA 273 METHOD [7]

The procedure given in this section is applicable to any type of masonry infill, i.e. existing masonry infill, enhanced panel for seismic rehabilitation and new panel added to an existing frame. All types of masonry infill panels shall be considered as primary elements of lateral force resisting system. Stiffness contribution of unreinforced masonry infill shall be represented as an equivalent compression strut. The strut has the same thickness and modulus of elasticity as the infill panel it represents. And the equivalent width, a , can be determined by,

$$a = 0.175 \cdot (\lambda_1 \cdot h_{col})^{-0.4} \cdot r_{inf} \quad (2.3)$$

where;

$$\lambda_1 = \left[\frac{E_{inf} \cdot t_{inf} \cdot \sin(2\theta)}{4 \cdot E_{fr} \cdot I_{col} \cdot h_{inf}} \right]^{\frac{1}{4}} \quad (2.4)$$

where;

h_{col} : Column height between centerlines of beam

h_{inf} : Height of infill panel

E_{fr} : Expected modulus of elasticity of frame material

E_{inf} : Expected modulus of elasticity of infill materials

I_{col} : Moment of inertia of column

r_{inf} : Diagonal length of infill panel

t_{inf} : Thickness of infill panel and equivalent strut

θ : Angle whose tangent is the infill height-to-length aspect ratio, in radians.

As in Smith & Carter's [6] method, the equivalent strut width is related with non-dimensional parameter, $\lambda_1 h_{col}$.

2.3 FAILURE MODES OF MASONRY INFILLED R/C FRAMES

Depending on relative properties of frame and infill, failure modes of masonry infilled frame show variety. In other words, failure can occur in the frame elements or in the infill. In estimating the lateral strength and lateral stiffness of masonry infilled frame, it is necessary to find the most critical of the various modes of failure of the frame and infill.

The usual modes for frame failure are tension failure of surrounding column elements or shear failure of the columns or beams. These modes are given in Figure 2.4 (Taken from [5]). Tension failure of the column results from applied overturning moments. Such mode may be critical one in infilled frames with high aspect ratio and with very rigid frame elements. The tension steel acts as a flange of the composite wall. However, in case of weak frame element, dominant modes of failures are flexural or shear failure of column or beams at plastic hinge locations.

However, if the frame strength is enough to withstand, increasing lateral load results in failure of infill. In addition to that, the failure may be a sequential combination of the failure modes of frame and infill. For example, flexural or shear failure of the columns will generally follow a failure of infill. In both case, failure modes of infill show variety depending on geometric and material properties. Failure of the infill occurs by one of the following modes;

- a) Shear cracking along the interface between the bricks and mortar
- b) Tension cracking through the mortar joints and masonry
- c) Local crushing of the masonry or mortar in compression corner of the infill.

Failure modes of infill are presented in Figure 2.5 (Taken from [5]).

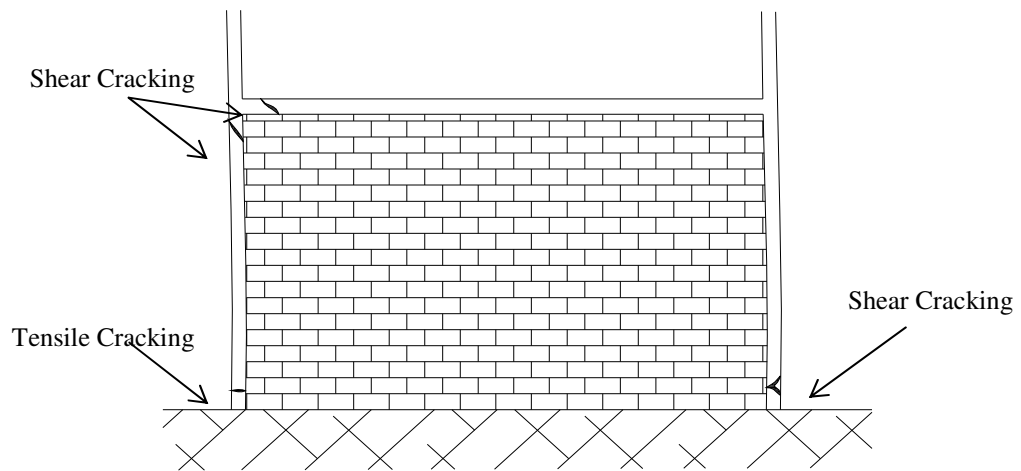


Figure 2.4 - Failure Modes of Reinforced Concrete Frame. (taken from [5])

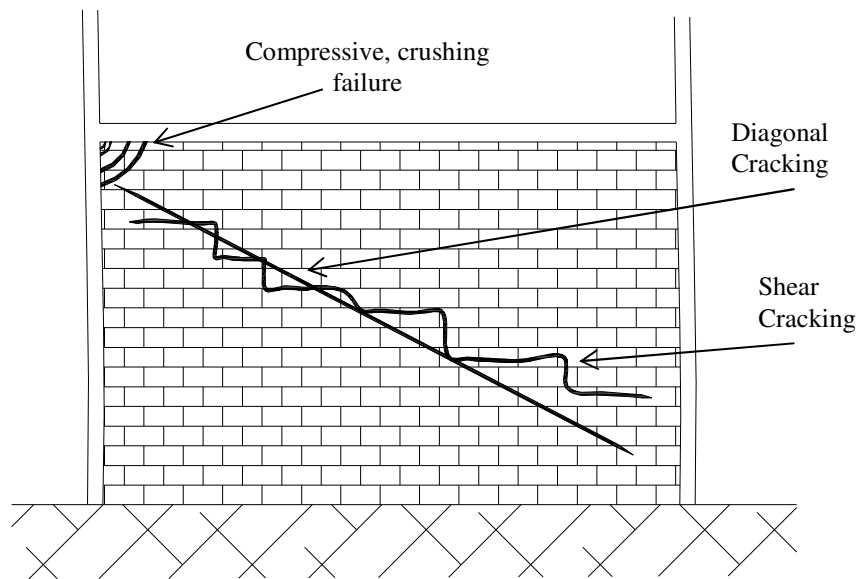


Figure 2.5 - Failure Modes of Infill. (taken from [5])

Shear failure of infill is directly related with the horizontal shear induced in the infill panel by applied load. In addition to applied load, shear resistance of masonry plays an important role. The resistance of masonry to shearing stress is usually considered to be provided by the combined action of the bond shear strength and the friction between the masonry and mortar. Also, vertical compressive stress level induced in infill panel by applied load is important. When a vertical compressive stress is applied to masonry the shear resistance is increased with the increase of friction between the masonry and the mortar. However, friction effect is less effective for the case of perforated brick. Test results [9] showed that for perforated brick the coefficient of internal friction, μ , is about 0.15, while it varies between 0.6 to 1.7 for solid brick.

Diagonal tension cracking is the result of the diagonal force which produces a principle tensile stress in the infill equal to tensile strength of the infill material. Smith and Carter [6] derived the lateral force cause diagonal crack on infill in terms of contact length between frame and infill under the light of their experimental results. This relation showed that greater value of the length to height ratio of infill or smaller value of λh (stiffer column relative to the infill) result in greater diagonal strength of infill.

Compressive failure of infill is accompanied by a rapidly increasing rate of deflection. Therefore, it can be said that compressive failure is a plastic type of infill failure. As done for diagonal tension failure, compressive failure load is related with the contact length between frame and infill by Smith & Carter [6] according to experimental results. The result of this relation can be concluded as follows; smaller value of λh results in greater compressive strength of infill. This can be explained with that stiffening of column leads to the reduction in lateral deflection. And stiffer column means smaller value of λh . However, because of the weakness of the shearing and tensile modes relative to the compressive failure mode, it is thought that a compressive failure would be unlikely to occur in brickwork.

Apart from these three modes of failure, a fourth mode of failure may take place. This is sliding shear failure. If sliding shear failure of the masonry infill occurs, the equivalent structural mechanism changes from the diagonally braced pin-jointed frame to the knee-braced frame. Therefore, this type mechanism results in shear failure of surrounding columns. This mechanism is shown in Figure 2.6 (Taken from [4])

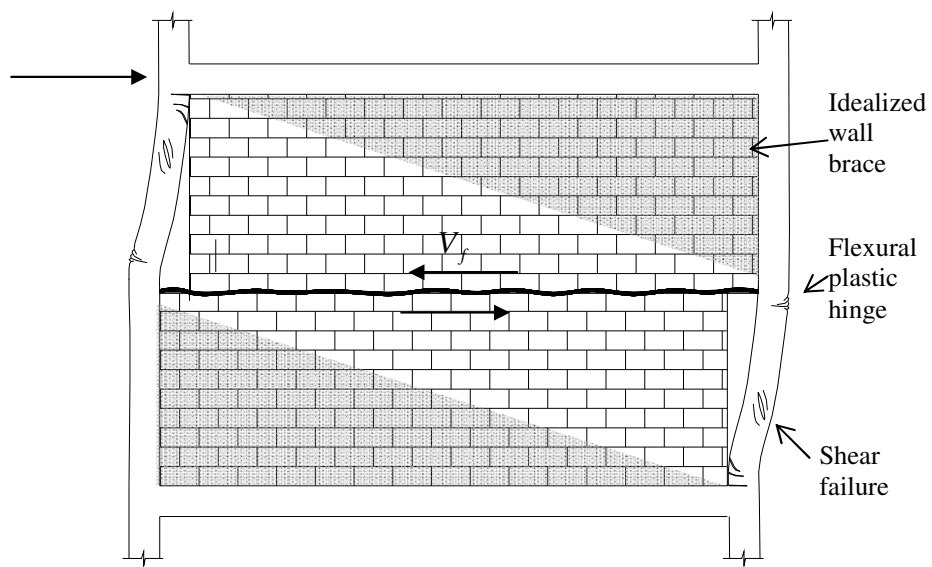


Figure 2.6 – Sliding Shear Failure of Infill. (taken from[4])

CHAPTER 3

DESCRIPTION AND ANALYSIS OF CASE STUDY BUILDINGS

3.1 INTRODUCTION

The theoretical approaches given in Chapter II are applied in two case studies. It is aimed to understand the behavior of structure modeled with the inclusion of masonry infill wall. Moreover, the two approaches to determining the compression strut width, Smith & Carter [6] method and FEMA 273 [7] method are also compared with each other.

Two different buildings were selected to investigate the effect of various parameters on the seismic performance. First, the structural properties of the buildings that are the subject of Case I and Case II are described with their layouts. Then earthquake loads assigned to the buildings are determined with respect to provisions given in Turkish Seismic Code (ABYYHY 98) [1]. After that, the analyses performed in both cases are explained in detail. Modeling assumptions, parameters and their ranges considered in analysis phases are presented. Finally, the results of sample analysis are given.

3.2 DESCRIPTION OF CASE STUDY BUILDINGS

3.2.1 CASE I – THREE STORY BUILDING

The building that is the first case is based on a real structure used as an office building. It has a symmetrical layout and consists of three stories with typical story height of 3.6 m. Floor plan of all stories is rectangular having 49.94 m length in x-direction and 12.72 m length in y-direction. The typical floor plan is shown in Figure 3.1.

Structural system consists of nine frames in short direction and four frames in long direction. Frames in short direction have three bay widths of 5.12, 2.18 and 5.12 m, respectively, while frames in long direction include eight bays having equal width of 6.12 m. The typical frames in x- and y- directions are given in Figure 3.2. The columns are located at the axes intersections. Beams in short direction and in long direction at all stories are 30 cm by 45 cm size. Also reinforced concrete slab has 15 cm of thickness.

There are no irregularities in structural system configuration. Also, the arrangement of the masonry infill does not disturb the symmetric floor plan of the building. Location of partition and outer walls are also shown in Figure 3.1. It is aimed to satisfy the floor symmetry with the arrangement of the infill walls, also.

Table 3.1 - Compression Strut Properties for Case I (Initial Model)

DIR	Ec (Mpa)	Em (Mpa)	b (m)	h (m)	t (cm)	Comp.Strut Widht (cm)	
						SMITH	FEMA
X	26150	700	6,12	3,60	20	90	70
Y	26150	700	5,12	3,60	20	70	60

For this model, compression struts are located with the properties given in Table 3.1.

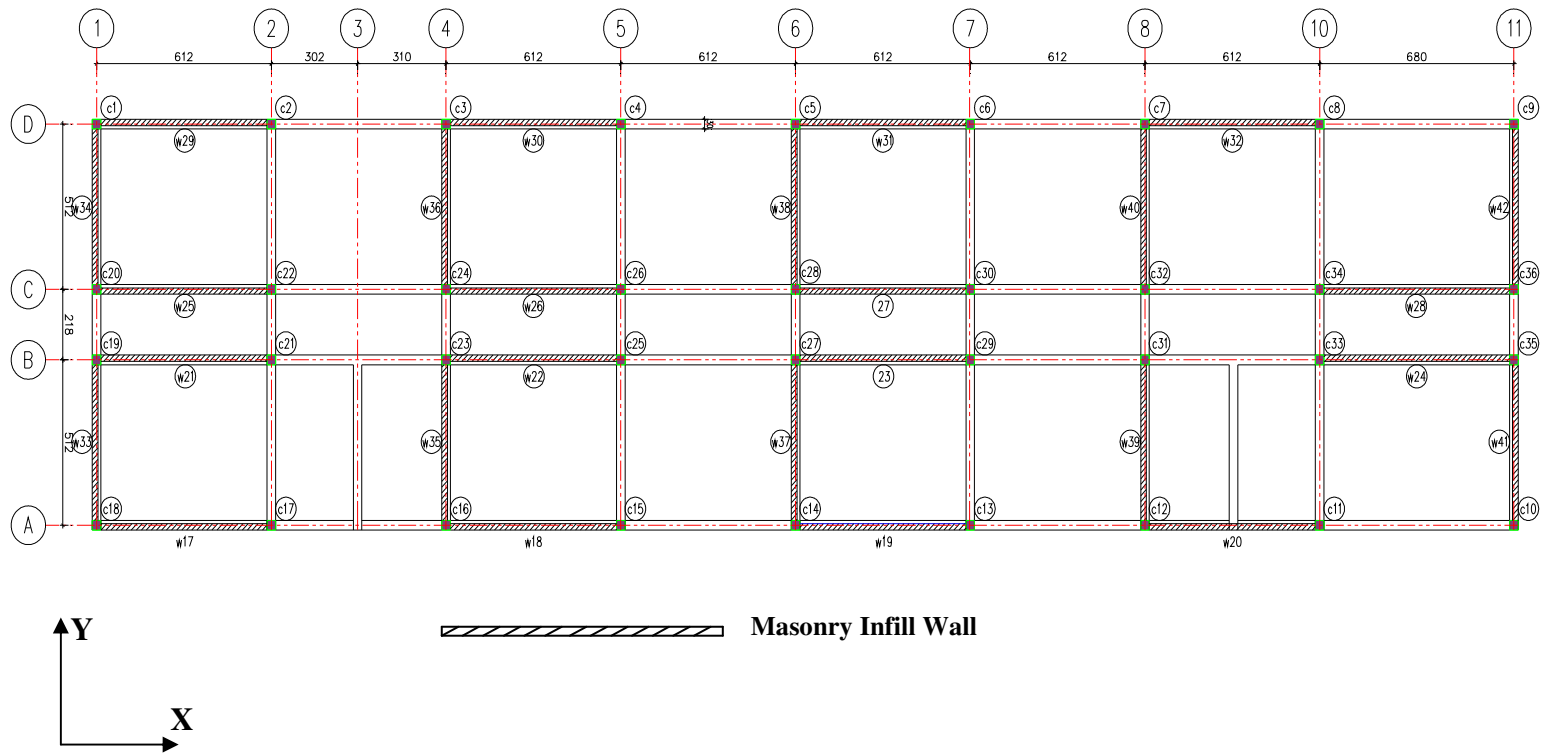
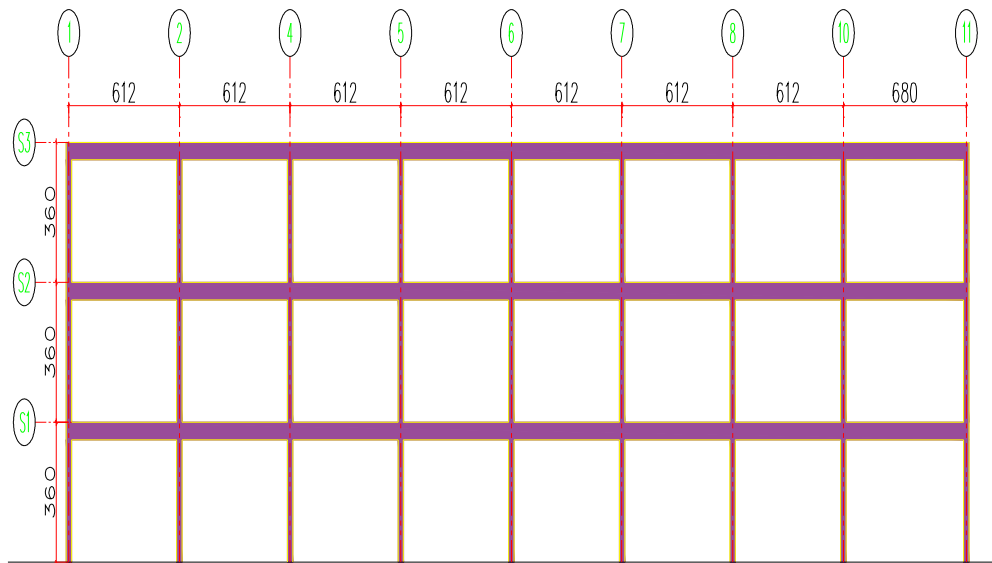
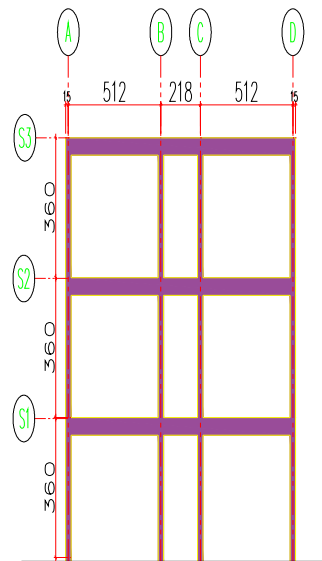


Figure 3.1 - Typical Floor Plan for Case I



All dimensions are in cm



All dimensions are in cm

Figure 3.2 - Frame in X and Y-direction for Case I.

3.2.2 CASE II – SIX STORY BUILDING

The building that is second case of this study is a generic structure. It has a symmetrical floor plan and consists of six stories with typical story height of 3.6 m. Floor plan of all stories is rectangular having 49.94 m length in x-direction and 24.94 m length in y-direction. The typical floor plan is shown in Figure 3.3.

Structural system consists of nine frames in short direction and seven frames in long direction. Frames in short direction have six bays having width of 5.12, 2.18, 5.02, 5.02, 2.18 and 5.12 m respectively, while frames in long direction include eight bays having equal width of 6.12 m. Elevation views in x- and y- directions are given in Figure 3.4. The columns are located at the axes intersections. Beams in short direction and in long direction at all stories are 40 cm by 50 cm size. Also reinforced concrete slab is having 15 cm of thickness.

This building, like Case I, has no irregularity in structural system. The locations of masonry infill wall, shown in Figure 3.3, are selected to maintain the floor symmetry. Since the bay widths and the column sizes are different from Case I, compression strut widths are also different for Case II. Compression strut properties for Case II are given in Table 3.2.

Table 3.2 - Compression Strut Properties for Case II (Initial Model)

DIR	Ec (Mpa)	Em (Mpa)	b (m)	h (m)	t (cm)	Comp.Strut Widht (cm)	
						SMITH	FEMA
X	26150	700	6,12	3,60	20	90	95
Y	26150	700	5,12	3,60	20	75	80

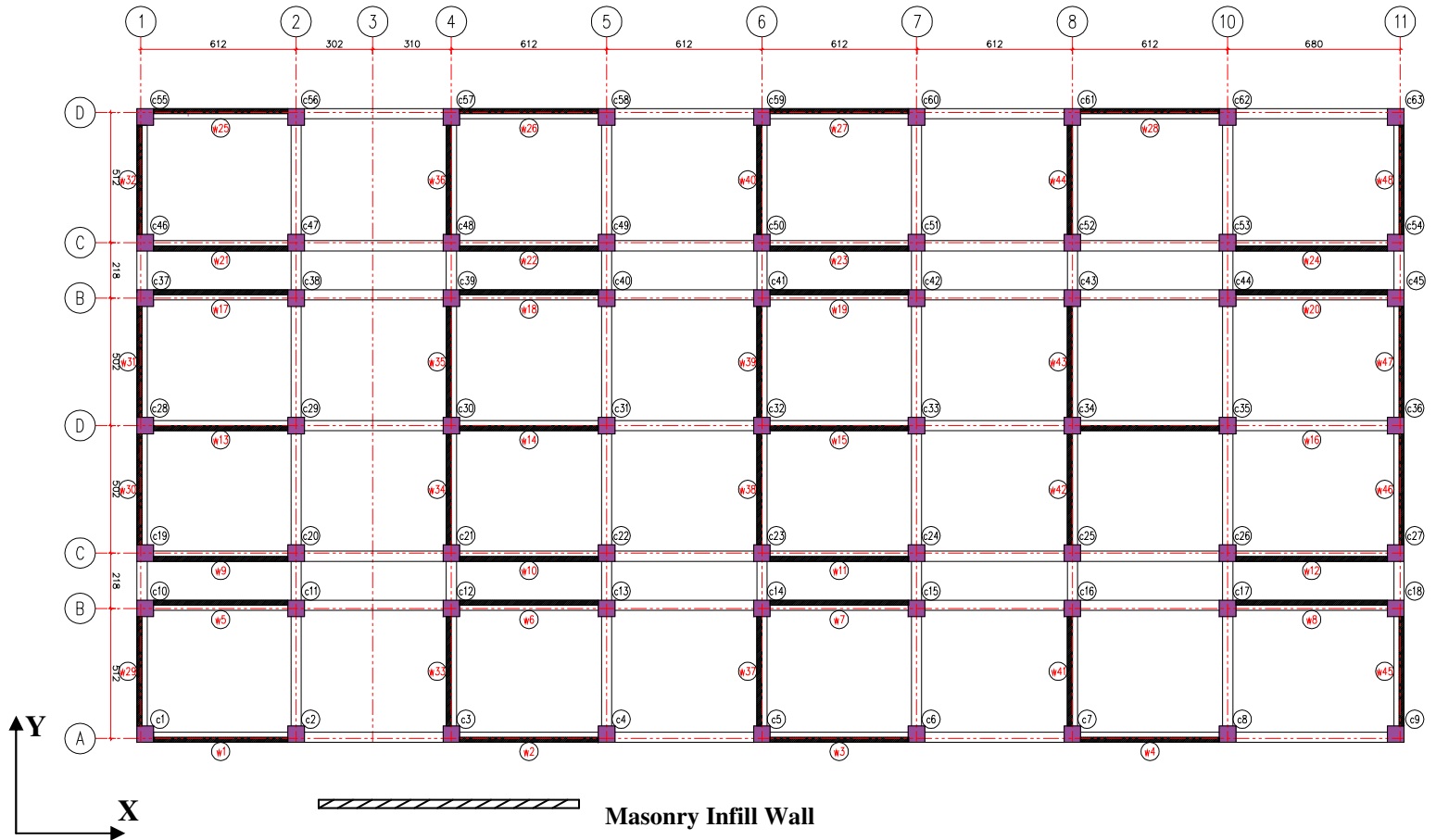
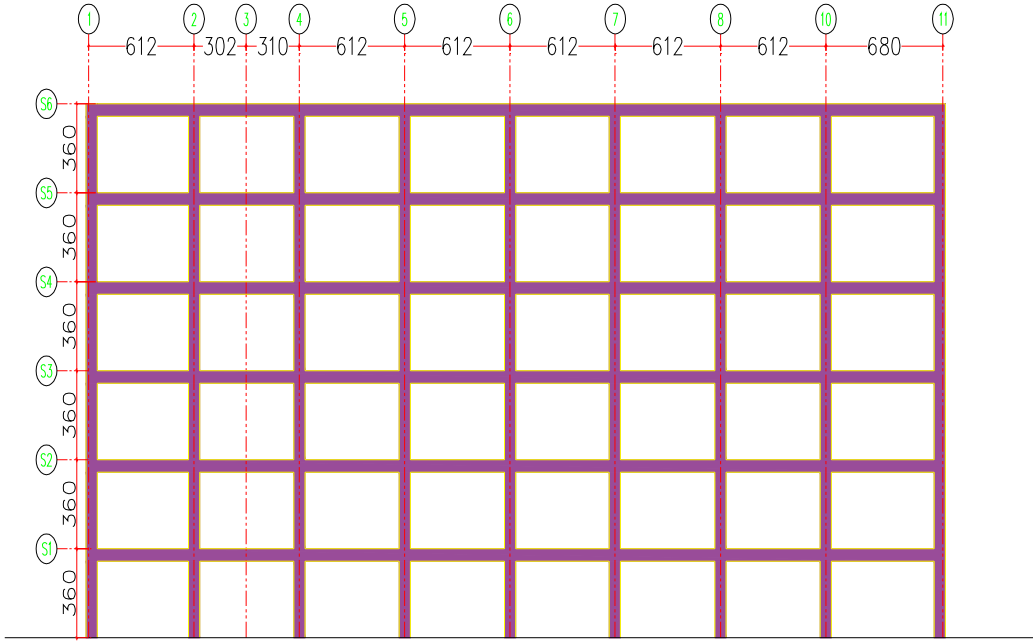
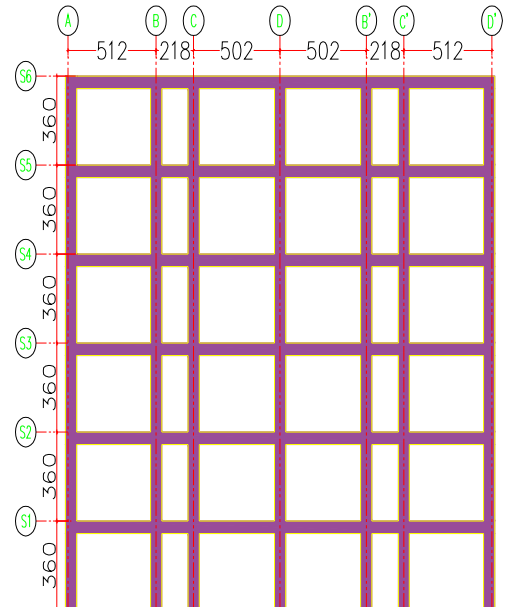


Figure 3.3 - Typical Floor Plan for Case II



All dimensions are in cm



All dimensions are in cm

Figure 3.4 - Frame in X and Y-direction for Case II

3.3 ANALYSIS OF BUILDINGS

3.3.1 MODELING ASSUMPTIONS

All models that are developed to determine the effect of masonry infill wall on seismic performance of the building were created in commercial programs SAP2000 (Structural Analysis Program) [10] and ETABS [8]. While creating 3-D models, some basic assumptions were taken into account to decrease the complexity of the problem and the analysis run time. Also, it is known that there are lots of parameters that have effects on the behavior of building system under loading, especially earthquake loading. At the beginning stage, these complexities were also tried to be minimized with the selection of the proper structural systems and building properties. Material properties of concrete and masonry are fixed for both cases. Material properties of concrete are listed in Table 3.3.

Table 3.3 – Concrete Material Properties

Concrete Class		Compression Strength, f_{ck}		Tensile Strength, f_{ctk}		Elastic Modulus, E_{c28}	
CEB	TS-500	MPa	(kgf/cm ²)	MPa	(kgf/cm ²)	MPa	(kgf/cm ²)
C14	BS14	14	(140)	1,3	(13)	26150	(261500)

Taken from [11]

Masonry is the other material used in models. Masonry has variable material properties. FEMA 273 [7] describes masonry in detail as mentioned in Chapter 2. According to FEMA 273 [7], masonry can be classified into three conditions;

- Masonry in good condition; $f_{inf} \leq 6MPa$
- Masonry in fair condition; $f_{inf} \leq 4.MPa$
- Masonry in poor condition; $f_{inf} \leq 2MPa$

In this study, the mechanical properties of the masonry walls were determined based on the tests performed in [12]. Accordingly mean compressive strength of the masonry is taken as 1 *MPa* and the modulus of elasticity is considered as 700 *MPa*.

Element assignment of prepared analysis models are done with the help of the template properties of ETABS [8]. All frame elements, such as columns and beams are modeled as a line element with six degrees of freedom. Instead of defining the reinforced concrete slab as an area element, it is preferred that reinforced concrete slab is modeled as a rigid diaphragm.

Another element in the models is compression strut representing the masonry wall. Strut dimensions are determined according to the methods described in Chapter 2. The important point from the element assignment point of view is connection of the strut with the frame. In the light of the Smith [9], the best approach is to model the compression strut as a pinned-end line element (Figure 3.5). Therefore, the struts contribute to the model axially in its direction of loading only.

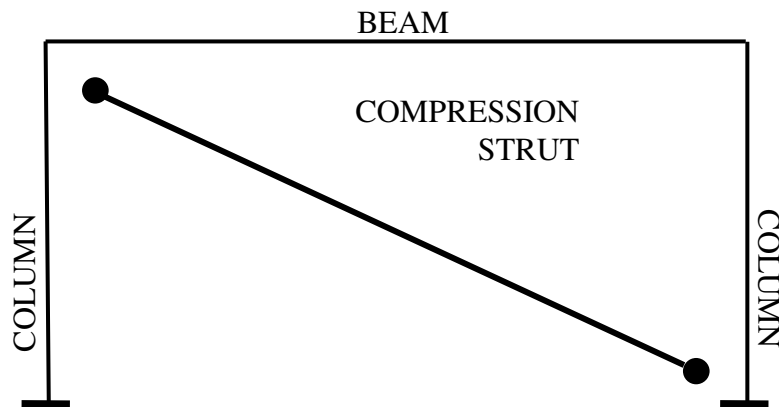


Figure 3.5 - Compression Strut Connection.

As a result, all frames in both x- and y- directions consist of line elements which have properties described above. Line element, representing columns and beams, are assigned end offset with rigid zone factor and elements representing masonry walls are assigned moment release at both ends. Material properties of concrete are assigned to column and beams and material properties of masonry is assigned to the compression struts. However, concrete slab is not modeled as an area element. Instead of assigning area element, rigid diaphragm is assigned to all joints at same story level. Thus, the number of degree of freedom decreases.

3.3.2 LINEAR ANALYSIS PROCEDURE

This study is mainly concerned with seismic performance, therefore vertical load analysis is not carried out. The models are subjected to earthquake load only.

There are different ways to carry out the earthquake load analysis of a design model. Time history analysis or response spectrum analysis can be performed. Moreover these types of analyses can be performed non-linearly. But, if the structure has convenient properties, which are described in Turkish Seismic Code (ABYYHY-98) [1], to apply the static equivalent seismic load method, this method is the simplest and the fastest way for analyzing the structure under the seismic action. The structures employed have a total height of 10.6 and 21.6 meters for Case I and Case II, respectively. Also, they have irregularities neither in plan nor in elevation. Therefore, they satisfy all requirements that are described in Turkish Seismic Code (ABYYHY-98) [1]. Therefore, static equivalent seismic load method is applicable for these structures.

According to this method, first the total weight of the structure must be determined. With the known weight of structure, the equivalent seismic load can be calculated and applied to the structure from the center of gravity. In the following paragraphs, calculation of equivalent seismic load for Case I and Case II buildings is explained separately.

3.3.2.1 CASE I

Equivalent earthquake load is calculated by using the procedure explained in ABYYHY-98 [1]. The first step is determining the total weight of structure. Concrete and masonry weights are taken as $2.5 t/m^3$ and $0.35 t/m^2$, respectively. Total weight consists of self weight of structure, finishing weight (taken as $0.2 t/m^2$), and live load. Live load is taken as $0.2 t/m^2$ for first and second stories. For the top floor, it is assumed that the snow load is $0.075 t/m^2$. By multiplying the value with floor area, snow load is calculated as 47.65 tons by using TS-498 [13]. Dead load components for one story are given in Table 3.4.

Table 3.4 - Dead Load Component for One Story for Case I

type	t (m)	b (m)	h (m)	l (m)	number	unit w. (t/m^3)	weight (ton)
Slab	0,15	49,94	12,72	-	1,00	2,50	365,26
Column	-	0,30	0,30	3,15	36,00	2,50	25,52
Beam	-	0,30	0,30	302,28	-	2,50	68,01
wall-x	0,20	5,82	3,15	-	16,00	1,88	110,00
wall-y	0,20	4,82	3,15	-	10,00	1,88	56,94

By using the equation given in [1], the story weights and total weight are also calculated. Total weight of structure, W , is calculated according to Equation 3.1 as a seismic weight. It consists of the summation of each story weight, w_i . The formula;

$$W = \sum_{i=1}^N w_i \quad (3.1)$$

The story weights in Equation 3.1 shall be calculated as;

$$w_i = g_i + n \cdot q_i \quad (3.2)$$

In the calculation of story weight, Dead load component acting on story i , g_i , such as column weights, slab weight, beam weights, covering weights, etc. are taken without any factor, but live loads components, q_i , are taken with the participation factor, n . For ordinary type of structures, live load participation factor, n , can be taken as 0.3.

Story weights are as follows;

Table 3.5 - Story Weights for Case I

Story ID	Dead L. (ton)	n	Live L. (ton)	Story Weight (ton)
3	529,50	0,30	47,64	543,79
2	625,72	0,30	127,05	663,84
1	529,50	0,30	127,05	567,62
TOTAL WEIGHT, W				1775,24

The equation of total base shear given in Equation 3.3

$$V_t = W \cdot A(T_1) / R_a(T_1) \geq 0.10 \cdot A_0 \cdot I \cdot W \quad (3.3)$$

where;

V_t : Total Base Shear

W : Total Weight of Structure

$A(T_1)$: Spectral Acceleration Coefficient

$R_a(T_1)$: Seismic Load Reduction Factor

A_0 : Effective Ground Acceleration Coefficient

I : Building Importance Factor

Applied static lateral force at each story level can be calculated by using $W, A_0 = 0.4, I = 1.0, S(T_1) = 2.5$ and $R(T_1) = 1$.

$$V_t = \frac{(1775.24)(0.4)(1.0)(2.5)}{1} = 1775.24 \text{ ton}$$

Total base shear is distributed to stories. Distribution of total base shear is represented in tabular form in Table 3.6.

Table 3.6 - Seismic Load Acting on Each Story (Case I)

Story ID	w_i (ton)	h_i (m)	$w_i h_i$	$w_i h_i / \sum w_i h_i$	$V_t * w_i h_i / \sum w_i h_i$
3	543,79	10,80	5872,95	0,46	821,20
2	663,84	7,20	4779,63	0,38	668,32
1	567,61	3,60	2043,41	0,16	285,72
Σ	1775,24		12695,99	1,00	1775,24

3.3.2.2 CASE II

Equivalent earthquake load is calculated by using the same procedure followed for Case I. The first step is to determine the total weight of structure. Concrete and masonry weights are taken as 2.5 t/m^3 and 0.35 t/m^2 , respectively as in Case I. Total weight consists of self weight of structure, finishing weight (taken as 0.2 t/m^2), and live load. Live load is taken as 0.2 t/m^2 for the first five stories. . For the top floor, it is assumed that the snow load is 0.075 t/m^2 . By multiplying the value with floor area, snow load is calculated as 93.41 tons by using TS-498 [13]. Dead load components for one story are given in Table 3.7.

Table 3.7 - Dead Load Component for one Story for Case II

type	t (m)	b (m)	h (m)	l (m)	number	unit w. (t/m ³)	weight (ton)
Slab	0,15	49,94	24,94	-	1	2,50	716,16
Column	-	0,65	0,65	3,10	63	2,50	206,29
Beam	-	0,40	0,35	548,84	-	2,50	192,09
wall-x	0,20	5,47	3,10	-	28	1,75	166,18
wall-y	0,20	4,37	3,10	-	20	1,75	94,83

The story weights and total weight are also calculated. In calculation, live load participation factor, n , is taken as 0.3. Story weights are as follows;

Table 3.8 - Story Weights for Case II

Story ID	Deal Load (ton)	n	Live Load (ton)	Story Weight (ton)
6	1141,91	0,30	93,41	1169,93
5	1375,55	0,30	249,10	1450,28
4	1375,55	0,30	249,10	1450,28
3	1375,55	0,30	249,10	1450,28
2	1375,55	0,30	249,10	1450,28
1	1141,91	0,30	249,10	1216,64
TOTAL WEIGHT, W				8187,69

Applied static lateral force at each story level can be calculated by using Equation 3.3. ($A_0 = 0.4, I = 1.0, S(T_1) = 2.5$ and $R(T_1) = 1$)

$$V_t = (8187.69)(0.4)(1.0)(2.5) = 8187.69 \text{ ton}$$

Total base shear is distributed to stories. Distribution of total base shear is represented in tabular form in Table 3.9.

Table 3.9 - Seismic Load Acting on Each Story (Case II)

Story ID	w_i (tons)	h_i (m)	$w_i h_i$	$w_i h_i / \sum w_i h_i$	$V_t * w_i h_i / \sum w_i h_i$
6	1169,93	21,6	25270,49	0,25	2013,80
5	1450,28	18,0	26105,04	0,25	2080,31
4	1450,28	14,4	20884,03	0,20	1664,24
3	1450,28	10,8	15663,02	0,15	1248,18
2	1450,28	7,2	10442,02	0,10	832,12
1	1216,64	3,6	4379,90	0,04	349,03
V_t	8187,69	Σ	102744,50	1,00	8187,69

3.3.3 PARAMETERS CONSIDERED AND THEIR RANGES

In order to understand the effect of masonry infill wall, both Case I and Case II were analyzed with and without including the masonry infill walls. In addition, to compare different techniques in the infill wall analysis, both cases were analyzed by using Smith and Carter method [6] and FEMA 273 [7]. In summary, for each case building three different models were prepared. These are,

- The building consisting of only RC frame elements. (*FR*)
- The building consisting of RC frame elements and compression struts which are modeled according to Smith & Carter [6]. (*SM*)
- The building consisting of RC frame elements and compression struts which are modeled according to FEMA 273 [7]. (*FE*)

For both cases, effectiveness of different parameters on seismic behavior of such system is tried to be investigated. Column size, infill wall area and distribution of infill wall are considered as the parameters which may affect the behavior. However, their ranges and amounts for each case are different. The plan layouts, number of columns, number of axes in both directions are different. Before

describing the parameters in detail, two new parameters must be defined to minimize the confusion. These are Column Index, CI , and Wall Index, WI . These indexes are calculated separately in each direction of loading as given in Equations (3.4 a - d).

$$CI_x = \frac{A_{ce_x}}{A_s} \cdot 100 \quad (3.4a)$$

$$CI_y = \frac{A_{ce_y}}{A_s} \cdot 100 \quad (3.4b)$$

$$WI_x = \frac{A_{w_x}}{A_s} \cdot 100 \quad (3.4c)$$

$$WI_y = \frac{A_{w_y}}{A_s} \cdot 100 \quad (3.4d)$$

where, A_{ce_x} and A_{ce_y} are the effective column areas in x- and y- directions, respectively. A_{w_x} and A_{w_y} are wall area in x and y directions. A_s is the total floor area. The approach used in this study for calculating the effective column area is given in Equation (3.5)

$$A_{ce_{x,y}} = \sum_{i=1}^N (n_{ci_{x,y}} \cdot A_{ci}) \quad (3.5)$$

where, A_{ci} is the individual column area. n_{ci_x} and n_{ci_y} are the effectiveness factor of that column in x and y directions respectively. If b_{xi} is taken as a column dimension in x-direction and b_{yi} is taken as a column dimension in y-direction, the effectiveness factors are as follows;

$$n_{ci_x} = \frac{b_{xi}}{(b_{xi} + b_{yi})} \quad (3.6a)$$

$$n_{ci,y} = \frac{b_{yi}}{(b_{xi} + b_{yi})} \quad (3.6b)$$

Substituting Equation (3.6a), Equation (3.6b) and Equation (3.5) in Equation (3.4a)

$$CI_{x,y} = \frac{\sum_{i=1}^N \left(\frac{b_{xi,yi}}{b_{xi} + b_{yi}} \cdot A_{ci} \right)}{A_s} \cdot 100 \quad (3.7)$$

It is also important to note that while calculating the WI , the walls along the calculated direction were taken into account.

3.3.3.1 COLUMN SIZE

A column, as a part of lateral load carrying system, is the most important structural element. Any change in column properties directly affects the behavior of structure which consists of either bare frame or infilled frame. Moreover any change in column properties also affects the diagonal strut properties as mentioned earlier.

In Case I, column sizes of three story building are increased from 30 cm by 30 cm to 60 cm by 60 cm with the increment of 10 cm in each direction separately. In other words, column index is increased from 0.085 % to 0.340 % in both x- and y-directions.

While changing the column sizes, the wall thickness ($t = 20cm$) and wall arrangements are kept unchanged. However, compression strut widths show variation according to change in surrounding frame size and rigidity. In Table 3.10, the column sizes and corresponding compression strut widths both in x and y-direction for SM and FE are listed.

Table 3.10 - Compression Strut Widths for Different Column Sizes (Case I)

Column Sizes		Comp. Strut Width in X-dir		Comp. Strut Width in Y-dir	
b_x	b_y	<i>FE</i>	<i>SM</i>	<i>FE</i>	<i>SM</i>
(cm)	(cm)	(cm)	(cm)	(cm)	(cm)
30	30	70	90	60	70
30	40	75	90	65	75
30	50	75	90	70	75
30	60	80	90	75	75
40	30	80	90	65	75
40	40	80	90	70	75
40	50	75	90	70	75
40	60	85	90	75	75
50	30	80	90	65	75
50	40	85	90	70	75
50	50	85	90	75	75
50	60	90	90	75	75
60	30	85	90	65	75
60	40	90	90	70	75
60	50	90	90	75	75
60	60	90	90	80	75

For Case II, the same procedure is followed. Column sizes of the six story building are increased from 50 cm by 50 cm to 90 cm by 90 cm with the increment of 5 cm in each direction. In other words, the column index is increased from 0.105 % to 0.341 % in both x- and y- directions.

While changing the column sizes, the wall thickness ($t = 20\text{cm}$) and wall arrangements are kept unchanged. However, compression struts in models are affected by the change in column size. In Table 3.11, the column sizes and corresponding compression strut widths both in x and y-directions for *SM* and *FE* are listed.

Table 3.11 - Compression Strut Widths for Different Column Sizes (Case II)

Column Sizes		Comp. Strut Width in X-dir		Comp. Strut Width in Y-dir	
b_x	b_y	<i>FE</i>	<i>SM</i>	<i>FE</i>	<i>SM</i>
(cm)	(cm)	(cm)	(cm)	(cm)	(cm)
50	50	85	95	75	75
60	60	90	90	80	75
65	65	95	90	80	75
70	70	95	90	80	75
75	75	95	90	85	75
80	80	100	90	85	75
85	85	100	90	85	75
90	90	100	90	85	75

3.3.3.2 INFILL WALL AREA

The second parameter is the infill wall area. While the column area is kept constant, the wall dimensions are changed. Column sizes and layouts are fixed to 50 cm by 50 cm for Case I (three story building) and 65 cm by 65 cm for Case II (six story building). Wall thicknesses are increased from 20 cm to 35 cm step by step with the increment of 5 cm for both cases. In other words, wall index is increased from 0.93 % to 1.62 % and 0.46 % to 0.81 % in x- and y-directions, respectively for Case I and increased from 0.41 % to 0.72 % and 0.24 % to 0.41 % in x- and y- directions, respectively for Case II.

Any change in wall thickness has no effect on *FR* model. This means that, the drift ratio obtained from *FR* model since it contains RC frame elements only. This means that, the drift ratio obtained from *FR* model is constant for any change in infill wall thickness. On the other hand, *FE* model and *SM* model are directly affected by the change in wall thickness. The major effect is on the compression strut width. Compression strut widths for different wall thickness are listed for Case I and Case II in Table 3.12 and table 3.13 respectively.

Table 3.12 - Compression Strut Widths (Case I)

Wall Thickness t	Comp. Strut Width in X-dir		Comp. Strut Width in Y-dir	
	<i>FE</i>	<i>SM</i>	<i>FE</i>	<i>SM</i>
(cm)	(cm)	(cm)	(cm)	(cm)
20	85	90	75	75
25	85	90	75	75
30	85	90	70	75
35	80	90	70	75

Table 3.13 - Compression Strut Widths (Case II)

Wall Thickness t	Comp. Strut Width in X-dir		Comp. Strut Width in Y-dir	
	<i>FE</i>	<i>SM</i>	<i>FE</i>	<i>SM</i>
(cm)	(cm)	(cm)	(cm)	(cm)
20	95	90	80	75
25	90	90	80	75
30	90	90	80	75
35	90	90	75	75

3.3.3.3 ARRANGEMENT OF INFILL WALL

Arrangement of infill wall is another parameter which may affect the results. Three different models which have different wall arrangements are prepared for each case. In each case, the buildings used at previous phases are fundamental ones. These fundamental models are called as Model I. Other two models are modified versions of Model I, namely Model II and Model III. The applied modifications on Model I and followed analysis procedure are explained separately for each case in following paragraphs.

3.3.3.3.1 CASE I

In Case I, Model I is the model that is given in Figure 3.1. Some modifications are done on Model I to get different distribution of infill wall. In Model II, the walls lying on C axis in x-direction and lying on 6 axis in y-direction are omitted. In Model III, the walls lying on C and D axes in x-direction and lying on 4 and 8 axes are deleted. The important point of this operation is that the symmetry is tried to be maintained in all models, because disturbance of symmetry may results in additional effect on behavior. The differences between these models, namely Model I, Model II and Model III can be seen in the Figure 3.6.

In Model I, which is the fundamental model, wall thickness is increased from 20 cm to 35 cm step by step with the increment of 5 cm. To keep the total wall area constant in all three models, wall thicknesses of Model II and Model III are adjusted according to wall thickness of fundamental model. For example, in x-direction while there are sixteen 5.12 m length of wall element in fundamental model, in Model II there are twelve and in Model III there are eight of them. To satisfy equality of total wall area, wall thicknesses must be 1.33 times and 2.0 times larger than Model I in Model II and Model III, respectively, variation of wall thickness results in diversity of compression strut width. Wall thicknesses and corresponding compression strut widths for *FE* and *SM* are given in Table 3.14.

40

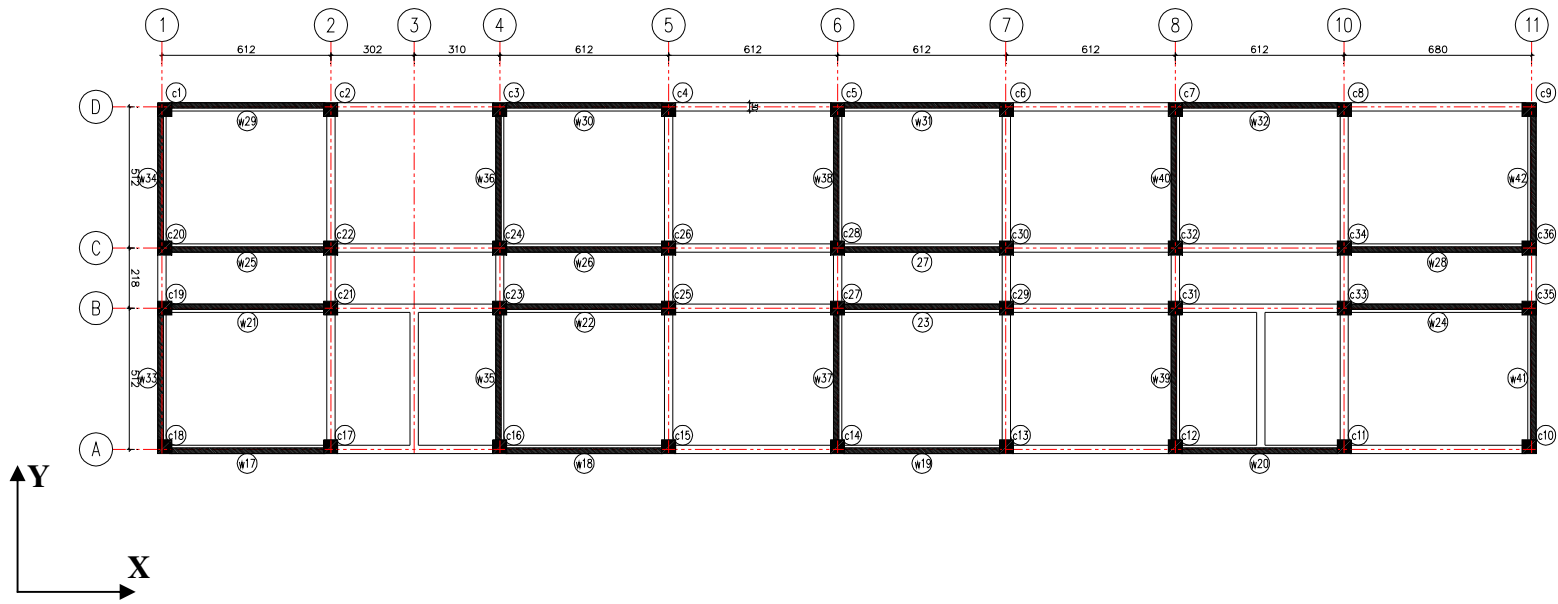


Figure 3.6a - Wall Arrangements of Model I for Case I

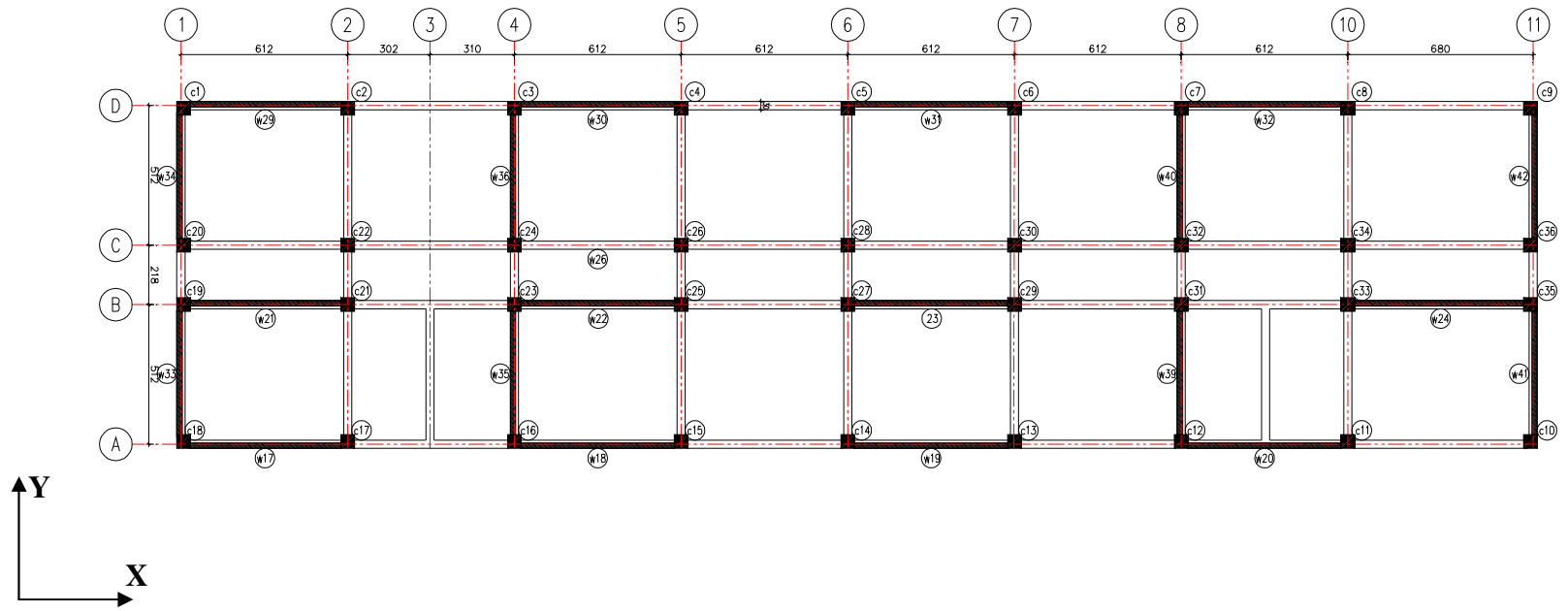


Figure 3.6b - Wall Arrangements of Model II for Case I

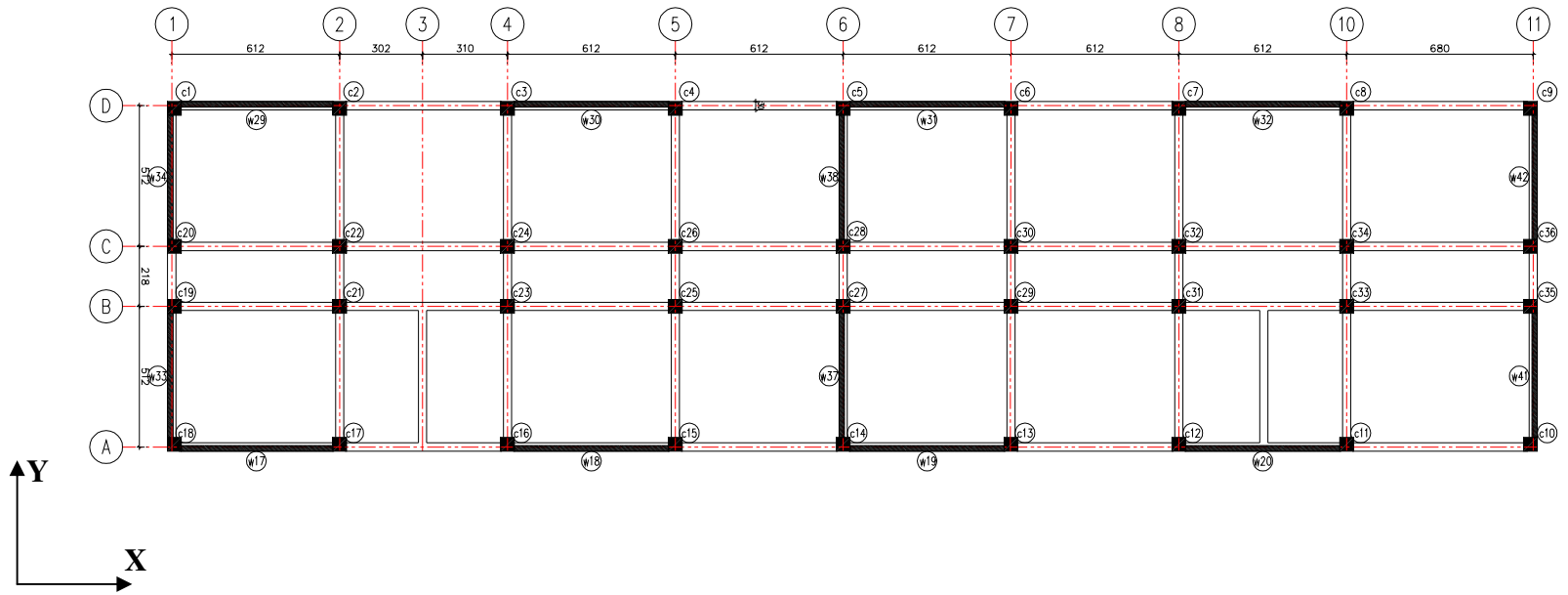


Figure 3.6c - Wall Arrangements of Model III for Case I

Table 3.14a - Wall Properties in X-direction (Case I)

Wall Thickness t	Model I			Model II			Model III		
	t	Comp. Strut Width in X-dir		t	Comp. Strut Width in X-dir		t	Comp. Strut Width in X-dir	
		FE	SM		FE	SM		FE	SM
(cm)	(cm)	(cm)	(cm)	(cm)	(cm)	(cm)	(cm)	(cm)	(cm)
20	20	85	90	26,67	85	90	40	80	90
25	25	85	90	33,33	80	90	50	80	90
30	30	85	90	40	80	90	60	75	90
35	35	80	90	46,67	80	90	70	75	90

Table 3.14b - Wall Properties in Y-direction (Case I)

Wall Thickness t	Model I			Model II			Model III		
	t	Comp. Strut Width in Y-dir		t	Comp. Strut Width in Y-dir		t	Comp. Strut Width in Y-dir	
		FE	SM		FE	SM		FE	SM
(cm)	(cm)	(cm)	(cm)	(cm)	(cm)	(cm)	(cm)	(cm)	(cm)
20	20	75	75	25	75	75	33,33	70	75
25	25	75	75	31,25	70	75	41,67	70	75
30	30	70	75	37,5	70	75	50	70	75
35	35	70	75	43,75	70	75	58,33	65	75

3.3.3.3.2 CASE II

In Case II, Model I is the model that is six story building given in Figure 3.4. Modified versions of fundamental model are also called as Model II and Model III as in Case I. In Model II, the walls lying on B and C' axes in x-direction and lying on 6 axis in y-direction are omitted. In model III, in addition the walls on B and C' axes, the walls lying on D axis in x-direction and instead of walls on 6 axis, the walls lying on 4 and 8 axes are omitted. Floor plans of three models are given in Figure 3.7.

As done for Case I, wall thickness is increased from 20 cm to 35 cm step by step with the increment of 5 cm in Model I. To keep the total wall area constant in all three models, wall thicknesses of Model II and Model III are adjusted according to wall thickness of fundamental model. For example, in x-direction while there are twenty eight 5.12 m length of wall element in fundamental model, in Model II there are twenty and in Model III there are sixteen of them. To satisfy equality of the total wall area, wall thicknesses of Model II and Model III must be 1.4 times and 1.75 times larger than wall thickness of Model I, respectively. Variation of wall thickness results in diversity of compression strut width. Wall thicknesses and corresponding compression strut widths for *FE* and *SM* are tabulated in Table 3.15.

45

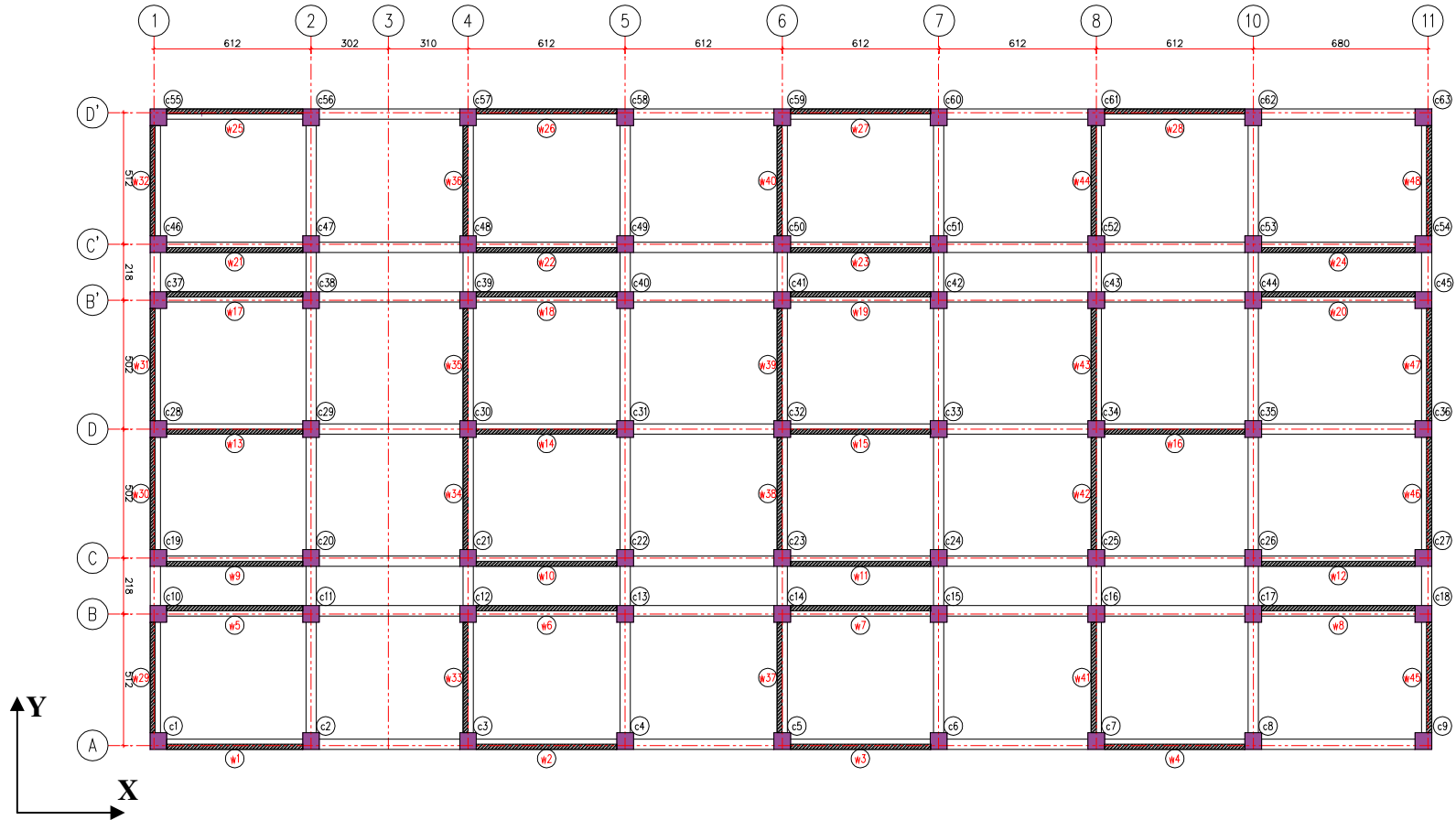


Figure 3.7a - Wall Arrangements of Model I for Case II

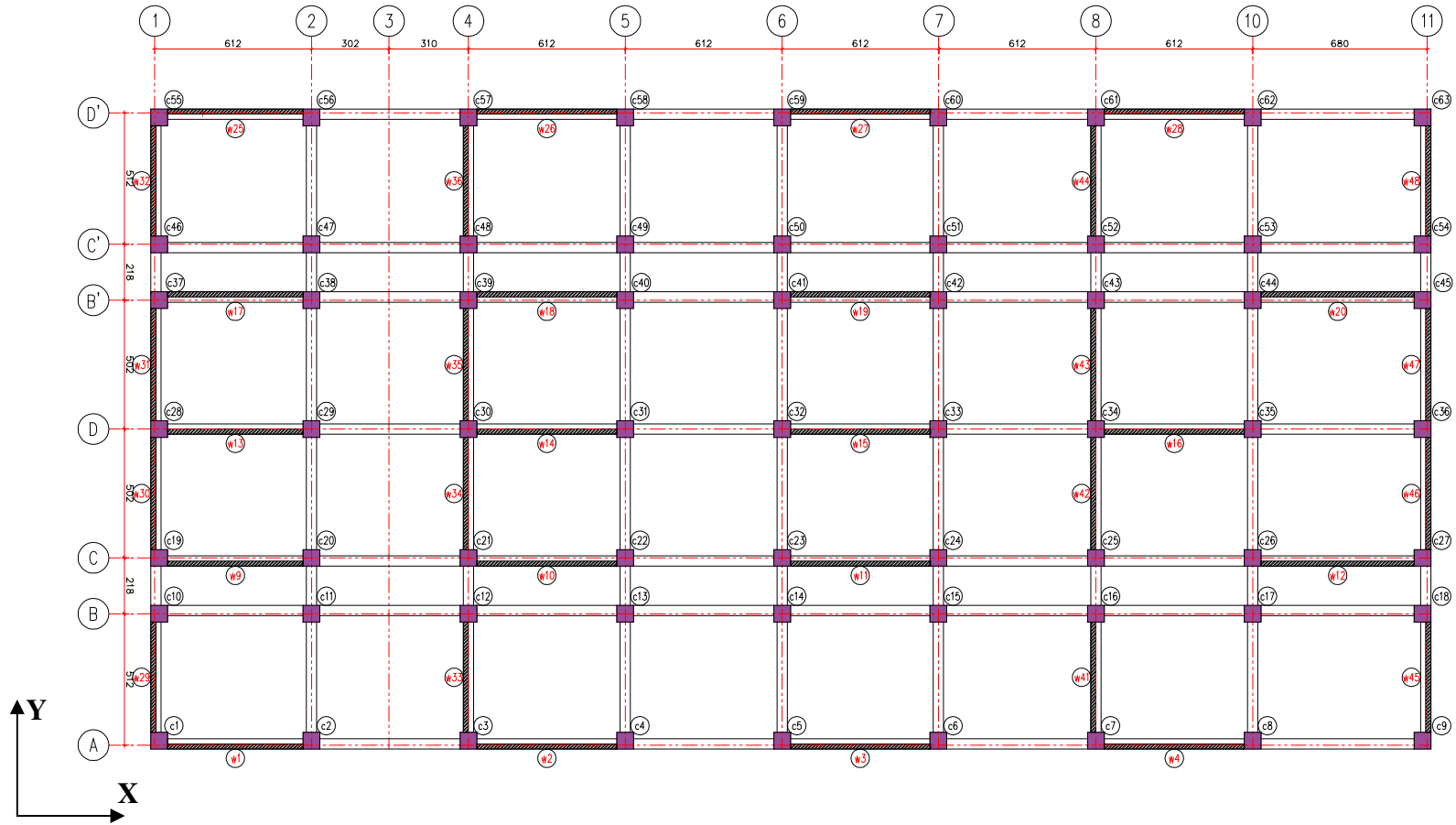


Figure 3.7b - Wall Arrangements of Model II for Case II

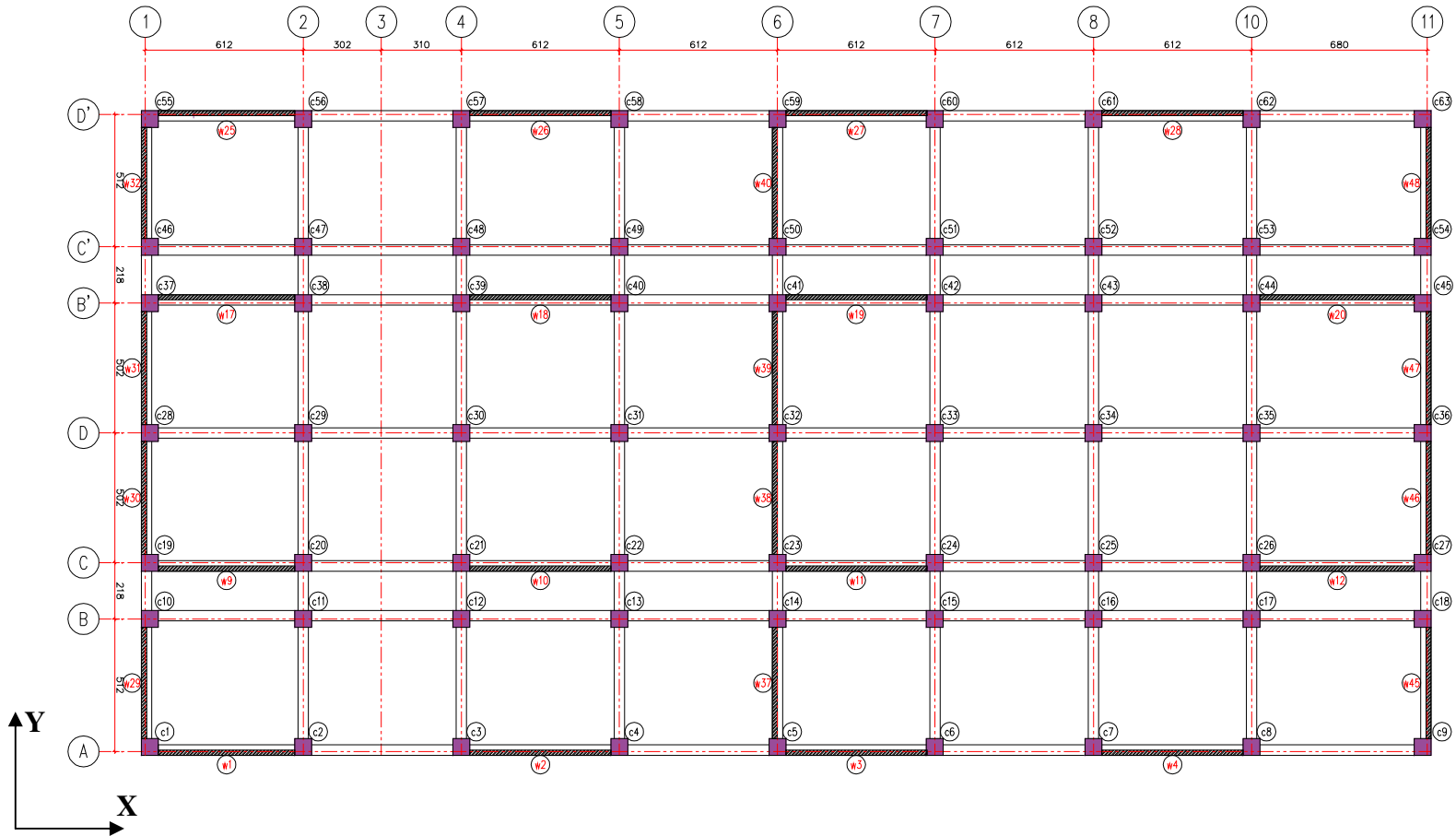


Figure 3.7c - Wall Arrangements of Model III for Case II

Table 3.15a - Wall Properties in X-direction (Case II)

Wall Thickness t	Model I			Model II			Model III		
	t	Comp. Strut Width in X-dir		t	Comp. Strut Width in X-dir		t	Comp. Strut Width in X-dir	
		FE	SM		FE	SM		FE	SM
(cm)	(cm)	(cm)	(cm)	(cm)	(cm)	(cm)	(cm)	(cm)	(cm)
20	20	95	90	28	90	90	35	90	90
25	25	90	90	35	90	90	43,75	90	90
30	30	90	90	42	90	90	52,5	85	90
35	35	90	90	49	85	90	61,25	85	90

Table 3.15b - Wall Properties in Y-direction (Case II)

Wall Thickness t	Model I			Model II			Model III		
	t	Comp. Strut Width in Y-dir		t	Comp. Strut Width in Y-dir		t	Comp. Strut Width in Y-dir	
		FE	SM		FE	SM		FE	SM
(cm)	(cm)	(cm)	(cm)	(cm)	(cm)	(cm)	(cm)	(cm)	(cm)
20	20	80	75	25	80	75	33,33	75	75
25	25	80	75	31,25	75	75	41,67	75	70
30	30	80	75	37,5	75	75	50	75	70
35	35	75	75	43,75	75	75	58,33	70	70

3.3.4 RESULTS OF SAMPLE ANALYSIS

The analysis results obtained from initial model for Case I building are discussed below. The sample analysis is performed on the building described in section 3.2 with column size 35 cm by 35 cm and with the layout given in Figure 3.1. Inter-story drift ratios, $\Delta_{i(\max)}/h_i$ are tabulated in Table 3.16. Including the masonry infill walls cause reduction in inter-story drift ratios. The ratio of $\Delta_{i(\max)}/h_i$ obtained from *FR* to *FE* and *SM* clarifies the reduction. Values are also shown in Table 3.16

Table 3.16 Inter-Story Drift Ratio for Sample Analysis

STORY	$\Delta_{ix(\max)}/h_i$			Reduction in $\Delta_{ix(\max)}/h_i$		$\Delta_{iy(\max)}/h_i$			Reduction in $\Delta_{iy(\max)}/h_i$	
	<i>FR</i>	<i>FE</i>	<i>SM</i>	$\frac{FR}{FE}$	$\frac{FR}{SM}$	<i>FR</i>	<i>FE</i>	<i>SM</i>	$\frac{FR}{FE}$	$\frac{FR}{SM}$
3	0,0220	0,0088	0,0076	2,49	2,88	0,0220	0,0120	0,0112	1,83	1,96
2	0,0390	0,0156	0,0134	2,50	2,91	0,0385	0,0212	0,0197	1,82	1,95
1	0,0382	0,0167	0,0145	2,28	2,64	0,0378	0,0223	0,0208	1,70	1,81

The results show that, masonry infill wall provides additional stiffness to the structure. This additional stiffness results in decrease of the lateral displacement. Reduction in the drift ratio in *SM* for all story that the reduction in the drift in *FE*. Also, reduction values decrease as the story level decreases. Such that, he reduction is about 2.5 for *FE* and 2.88 for *SM* at third story level, while they are about 2.28 for *FE* and 2.64 for *SM* at first story level.

It is also seen that, the story shears are shared between vertical frame elements and diagonal compression strut. Shear contribution of the compression struts and vertical frame element in all three case are shown in Table 3.17

Table 3.17a Shear Contribution of Elements in X-Direction

	FR	FE				SM			
story	$(V_{i-x})_{FR}$	$(V_{ci-x})_{FE}$	$\frac{(V_{ci-x})_{FE}}{(V_{i-x})_{FR}}$	$(V_{wi-x})_{FE}$	$\frac{(V_{wi-x})_{FE}}{(V_{i-x})_{FR}}$	$(V_{ci-x})_{SM}$	$\frac{(V_{ci-x})_{SM}}{(V_{i-x})_{FR}}$	$(V_{wi-x})_{SM}$	$\frac{(V_{wi-x})_{FE}}{(V_{i-x})_{FR}}$
	tons	tons		tons		tons		tons	
1	820,96	323,51	0,39	497,56	0,61	278,58	0,34	542,46	0,66
2	1489,00	580,79	0,39	908,29	0,61	496,23	0,33	992,84	0,67
3	1773,96	784,64	0,44	989,46	0,56	678,47	0,38	1095,68	0,62

Table 3.17b Shear Contribution of Elements in Y-Direction

	FR	FE				SM			
story	$(V_{i-y})_{FR}$	$(V_{ci-y})_{FE}$	$\frac{(V_{ci-y})_{FE}}{(V_{i-y})_{FR}}$	$(V_{wi-y})_{FE}$	$\frac{(V_{wi-y})_{FE}}{(V_{i-y})_{FR}}$	$(V_{ci-y})_{SM}$	$\frac{(V_{ci-y})_{SM}}{(V_{i-y})_{FR}}$	$(V_{wi-y})_{SM}$	$\frac{(V_{wi-y})_{FE}}{(V_{i-y})_{FR}}$
	tons	tons		tons		tons		tons	
1	821,00	449,69	0,55	371,31	0,45	420,25	0,51	400,76	0,49
2	1489,00	814,65	0,55	674,35	0,45	759,04	0,51	730,01	0,49
3	1773,99	1053,98	0,59	720,02	0,41	988,35	0,56	785,61	0,44

where;

$(V_{ci-x})_{FE}$: The shear carried by column at i. story in x-direction in *FE* .

$(V_{wi-x})_{FE}$: The shear carried by infill walls at i. story in x-direction in *FE* .

$(V_{ci-x})_{SM}$: The shear carried by column at i. story in x-direction in *SM* .

$(V_{wi-x})_{SM}$: The shear carried by infill walls at i. story in x-direction in *SM* .

$(V_{i-x})_{FR}$: Total shear at i. story in x-direction.

$(V_{ci-y})_{FE}$: The shear carried by column at i. story in y-direction in *FE* .

$(V_{wi-y})_{FE}$: The shear carried by infill walls at i. story in y-direction in *FE* .

- $(V_{ci-y})_{SM}$: The shear carried by column at i. story in y-direction in *SM* .
- $(V_{wi-y})_{SM}$: The shear carried by infill walls at i. story in y-direction in *SM* .
- $(V_{i-y})_{FR}$: Total shear at i. story in y-direction.

As expected, the results of sample analysis show that, infill walls have significant effect on shear load carrying system. Insufficient column size can be major reason for such an effective result. However, this effect is decreasing from top to bottom. Since the effective area of infill walls with respect to effective column area is greater in x- direction than that in y-direction, infill walls are more effective in x-direction than that in y-direction.

3.3.5 SUMMARY OF ANALYSES

In this study, totally 184 analyses were performed for different column sizes, wall areas and wall arrangements on 92 different models. All the building analyses performed are given in Table 3.18.

Table 3.18 Identification of Buildings

BUILDING ID.	CASE	MODEL TYPE	COLUMN SIZE (cm)		WALL THICKNESS (cm)	COLUMN INDEX		WALL INDEX		FRAME TYPE		
			b_x	b_y		t	CI_x	CI_y	WI_x	WI_y	FR	FE
B1	I	I	25	25	122	0,06	0,06	5,65	2,83		x	
B2	I	I	30	30	20	0,09	0,09	0,93	0,46	x	x	x
B3	I	I	30	30	32	0,09	0,09	1,48	0,74		x	
B4	I	I	30	30	97	0,09	0,09	4,50	2,25		x	
B5	I	I	30	40	20	0,10	0,13	0,93	0,46	x	x	x
B6	I	I	30	50	20	0,11	0,18	0,93	0,46	x	x	x
B7	I	I	30	60	20	0,11	0,23	0,93	0,46	x	x	x
B8	I	I	35	35	79	0,12	0,12	3,66	1,83		x	
B9	I	I	35	35	22	0,12	0,12	0,12	0,51		x	
B10	I	I	40	30	20	0,13	0,10	0,93	0,46	x	x	x
B11	I	I	40	40	14	0,15	0,15	0,65	0,33		x	
B12	I	I	40	40	20	0,15	0,15	0,93	0,46	x	x	x
B13	I	I	40	40	64	0,15	0,15	2,97	1,48		x	
B14	I	I	40	50	20	0,17	0,21	0,93	0,46	x	x	x
B15	I	I	40	60	20	0,18	0,27	0,93	0,46	x	x	x
B16	I	I	45	45	8	0,19	0,19	0,37	0,19		x	
B17	I	I	45	45	52	0,19	0,19	2,41	1,20		x	
B18	I	I	50	30	20	0,18	0,11	0,93	0,46	x	x	x
B19	I	I	50	40	20	0,21	0,17	0,93	0,46	x	x	x
B20	I	I	50	50	1	0,24	0,24	0,05	0,02		x	
B21	I	I	50	50	20	0,24	0,24	0,93	0,46	x	x	x
B22	I	I	50	50	25	0,24	0,24	1,16	0,58	x	x	x
B23	I	I	50	50	30	0,24	0,24	1,39	0,70	x	x	x
B24	I	I	50	50	35	0,24	0,24	1,62	0,81	x	x	x
B25	I	I	50	50	42	0,24	0,24	1,95	0,97		x	
B26	I	I	50	50	100	0,24	0,24	4,63	2,32		x	
B27	I	I	50	60	20	0,26	0,31	0,93	0,46	x	x	x
B28	I	I	55	55	35	0,29	0,29	1,62	0,81		x	
B29	I	I	55	55	95	0,29	0,29	4,40	2,20		x	
B30	I	I	60	30	20	0,23	0,11	0,93	0,46	x	x	x
B31	I	I	60	40	20	0,27	0,18	0,93	0,46	x	x	x
B32	I	I	60	50	20	0,31	0,26	0,93	0,46	x	x	x
B33	I	I	60	60	20	0,34	0,34	0,93	0,46	x	x	x
B34	I	I	60	60	26	0,34	0,34	1,20	0,60		x	
B35	I	I	60	60	84	0,34	0,34	3,89	1,95		x	
B36	I	I	65	65	21	0,40	0,40	0,97	0,49		x	
B37	I	I	65	65	72	0,40	0,40	3,34	1,67		x	

Table 3.18 (Continued) Identification of Buildings

BUILDING ID.	CASE	MODEL TYPE	COLUMN SIZE (cm)		WALL THICKNESS (cm)	COLUMN INDEX		WALL INDEX		FRAME TYPE		
			b_x	b_y		t	CI_x	CI_y	WI_x	WI_y	FR	FE
B38	I	I	70	70	15	0,46	0,46	2,09	1,04		x	
B39	I	I	70	70	63	0,46	0,46	8,76	4,38		x	
B40	I	I	75	75	9	0,53	0,53	1,25	0,63		x	
B41	I	I	75	75	54	0,53	0,53	7,51	3,76		x	
B42	I	I	80	80	4	0,60	0,60	0,56	0,28		x	
B43	I	I	80	80	44	0,60	0,60	6,12	3,06		x	
B44	I	I	85	85	35	0,68	0,68	4,87	2,41		x	
B45	I	I	90	90	26	0,77	0,77	3,61	1,81		x	
B46	I	II	50	50	20	0,24	0,24	2,78	1,39		x	x
B47	I	II	50	50	25	0,24	0,24	3,48	1,74		x	x
B48	I	II	50	50	30	0,24	0,24	4,17	2,09		x	x
B49	I	II	50	50	35	0,24	0,24	4,87	2,44		x	x
B50	I	III	50	50	20	0,24	0,24	2,78	1,39		x	x
B51	I	III	50	50	25	0,24	0,24	3,48	1,74		x	x
B52	I	III	50	50	30	0,24	0,24	4,17	2,09		x	x
B53	I	III	50	50	35	0,24	0,24	4,87	2,44		x	x
B54	II	I	50	50	20	0,11	0,11	2,48	1,42	x	x	x
B55	II	I	50	50	21	0,11	0,11	2,61	1,49		x	
B56	II	I	55	55	14	0,13	0,13	1,74	0,99		x	
B57	II	I	55	55	50	0,13	0,13	6,20	3,55		x	
B58	II	I	60	60	8	0,15	0,15	0,99	0,57		x	
B59	II	I	60	60	20	0,15	0,15	2,48	1,42	x	x	x
B60	II	I	60	60	40	0,15	0,15	4,96	2,84		x	
B61	II	I	65	65	4	0,18	0,18	0,50	0,28		x	
B62	II	I	65	65	20	0,18	0,18	2,48	1,42	x	x	x
B63	II	I	65	65	25	0,18	0,18	3,10	1,77	x	x	x
B64	II	I	65	65	30	0,18	0,18	3,72	2,13	x	x	x
B65	II	I	65	65	34	0,18	0,18	4,22	2,41		x	
B66	II	I	65	65	35	0,18	0,18	4,34	2,48	x	x	x
B67	II	I	70	70	1	0,21	0,21	0,12	0,07		x	
B68	II	I	70	70	20	0,21	0,21	2,48	1,42	x	x	x
B69	II	I	70	70	28	0,21	0,21	3,47	1,99		x	
B70	II	I	75	75	20	0,24	0,24	2,48	1,42	x	x	x
B71	II	I	75	75	23	0,24	0,24	2,85	1,63		x	
B72	II	I	75	75	90	0,24	0,24	11,17	6,39		x	

Table 3.18 (Continued) Identification of Buildings

BUILDING ID.	CASE	MODEL TYPE	COLUMN SIZE (cm)		WALL THICKNESS (cm)	COLUMN INDEX		WALL INDEX		FRAME TYPE		
			b_x	b_y		t	CI_x	CI_y	WI_x	WI_y	FR	FE
B73	II	I	80	80	19	0,27	0,27	0,39	0,22		x	
B74	II	I	80	80	20	0,27	0,27	0,41	0,24	x	x	x
B75	II	I	80	80	83	0,27	0,27	1,72	0,98		x	
B76	II	I	85	85	14	0,31	0,31	0,29	0,17		x	
B77	II	I	85	85	20	0,31	0,31	0,41	0,24	x	x	x
B78	II	I	85	85	75	0,31	0,31	1,55	0,89		x	
B79	II	I	90	90	10	0,34	0,34	0,21	0,12		x	
B80	II	I	90	90	20	0,34	0,34	0,41	0,24	x	x	x
B81	II	I	90	90	66	0,34	0,34	1,37	0,78		x	
B82	II	I	100	100	52	0,42	0,42	1,08	0,62		x	
B83	II	I	105	105	46	0,47	0,47	0,95	0,54		x	
B84	II	I	110	110	40	0,51	0,51	0,83	0,47		x	
B85	II	II	65	65	20	0,18	0,18	0,41	0,24		x	x
B86	II	II	65	65	25	0,18	0,18	0,52	0,30		x	x
B87	II	II	65	65	30	0,18	0,18	0,62	0,36		x	x
B88	II	II	65	65	35	0,18	0,18	0,72	0,41		x	x
B89	II	III	65	65	20	0,18	0,18	0,41	0,24		x	x
B90	II	III	65	65	25	0,18	0,18	0,52	0,30		x	x
B91	II	III	65	65	30	0,18	0,18	0,62	0,36		x	x
B92	II	III	65	65	35	0,18	0,18	0,72	0,41		x	x

All information about buildings which are used in this study can be seen in Table 3.18. For example the building, which has an identification code of B89, is analyzed as a bare frame structure (*FR*), an infilled frame structure by using FEMA 273 [7] (*FE*) and an infilled frame structure by using Smith and Carter [6] method. It is also seen that column sizes are 65 cm in both x- and y- directions and wall thickness is equal to 20 cm for B89.

CHAPTER 4

INTERPRETATION AND DISCUSSION OF RESULTS

4.1 INTRODUCTION

The main purpose of this study is to investigate the contribution of hollow masonry infill wall to the lateral strength and stiffness of reinforced concrete buildings. For this purpose, several analyses were performed on two case study buildings. The analyses are performed phase by phase to explore the effect of different parameters on the behavior. These parameters are column size, infill wall thickness and arrangement of infill walls. The results of all analyses for both cases are presented in this section.

The most important result that reflects the contribution of infill wall to the lateral stiffness is the global drift ratio. Global drift ratio can be described as the ratio of maximum lateral displacement, Δ_{\max} , of the building to its total height, h . Inter-story drift ratio is another important parameter that is described as the ratio of the maximum displacement of a given story, Δ_i , relative to the story below, Δ_{i-1} , to the story height, h_i . It is evident that global drift ratio and inter-story drift ratio give approximately same information about the behavior of the buildings selected, because of the symmetric and typical story plans. The only difference between them is that inter-story drift ratio gives different numerical value according to the location of the story whereas global drift ratio gives the average result. Therefore,

results presented and discussed in this section are based on the global drift ratio only.

4.2 EFFECT OF COLUMN SIZE

To investigate the effect of masonry infill wall on buildings having different column sizes, two case buildings were subjected to lateral forces. For both cases, constant wall thickness is taken as 20 cm. This means that, WI_x and WI_y are 0.93 and 0.46 respectively for Case I and they are 0.41 and 0.24 respectively for Case II. On the other hand, column index is increased from 0.09 % to 0.34 % for Case I and it is increased from 0.11 % to 0.34 % for Case II.

The global drift ratios of Case I and Case II are given in Table 4.1 and Table 4.2 respectively. By using these results, the values of global drift ratio obtained from FR , FE and SM versus column index are given on same graph for each case (Figure 4.1 to 4.2). The values in x-and y- direction are given in Figure 4.1a and Figure 4.1b respectively for Case I and those for Case II are given in Figure 4.2a and Figure 4.2 b.

Table 4.1 - Global Drift Ratios for Case I

BUILDING ID	CI_x	CI_y	WI_x	WI_y	$\Delta_{x(max)}/h$			$\Delta_{y(max)}/h$		
					<i>FR</i>	<i>FE</i>	<i>SM</i>	<i>FR</i>	<i>FE</i>	<i>SM</i>
B2	0,085	0,085	0,93	0,46	0,0331	0,0137	0,0118	0,0327	0,0185	0,0172
B5	0,097	0,130	0,93	0,46	0,0272	0,0121	0,0109	0,0183	0,0124	0,0118
B6	0,106	0,177	0,93	0,46	0,0236	0,0112	0,0102	0,0127	0,0093	0,0091
B7	0,113	0,227	0,93	0,46	0,0211	0,0103	0,0097	0,0099	0,0075	0,0075
B10	0,130	0,097	0,93	0,46	0,0193	0,0099	0,0093	0,0265	0,0157	0,0148
B12	0,151	0,151	0,93	0,46	0,0166	0,0090	0,0086	0,0154	0,0107	0,0105
B14	0,168	0,210	0,93	0,46	0,0149	0,0087	0,0081	0,0110	0,0083	0,0082
B15	0,181	0,273	0,93	0,46	0,0137	0,0078	0,0077	0,0087	0,0068	0,0068
B18	0,177	0,106	0,93	0,46	0,0139	0,0082	0,0078	0,0227	0,0143	0,0135
B19	0,210	0,168	0,93	0,46	0,0123	0,0074	0,0072	0,0136	0,0098	0,0096
B21	0,236	0,236	0,93	0,46	0,0112	0,0069	0,0066	0,0099	0,0075	0,0075
B27	0,258	0,309	0,93	0,46	0,0105	0,0065	0,0065	0,0079	0,0063	0,0063
B30	0,227	0,113	0,93	0,46	0,0112	0,0069	0,0068	0,0201	0,0132	0,0125
B31	0,272	0,181	0,93	0,46	0,0100	0,0063	0,0063	0,0123	0,0091	0,0089
B32	0,309	0,258	0,93	0,46	0,0092	0,0059	0,0059	0,0091	0,0070	0,0070
B33	0,340	0,340	0,93	0,46	0,0086	0,0056	0,0056	0,0073	0,0058	0,0059

Table 4.2 - Global Drift Ratios for Case II

BUILDING ID	CI_x	CI_y	WI_x	WI_y	$\Delta_{x(max)}/h$			$\Delta_{y(max)}/h$		
					<i>FR</i>	<i>FE</i>	<i>SM</i>	<i>FR</i>	<i>FE</i>	<i>SM</i>
B54	0,105	0,105	0,41	0,24	0,0227	0,0154	0,0151	0,0196	0,0152	0,0152
B59	0,152	0,152	0,41	0,24	0,0180	0,0128	0,0128	0,0148	0,0119	0,0120
B62	0,178	0,178	0,41	0,24	0,0166	0,0118	0,0120	0,0133	0,0109	0,0110
B68	0,207	0,207	0,41	0,24	0,0154	0,0111	0,0113	0,0122	0,0101	0,0102
B70	0,237	0,237	0,41	0,24	0,0145	0,0106	0,0107	0,0114	0,0094	0,0096
B74	0,270	0,270	0,41	0,24	0,0136	0,0099	0,0102	0,0106	0,0089	0,0090
B77	0,305	0,305	0,41	0,24	0,0128	0,0095	0,0097	0,0100	0,0084	0,0086
B80	0,341	0,341	0,41	0,24	0,0121	0,0091	0,0093	0,0094	0,0080	0,0081

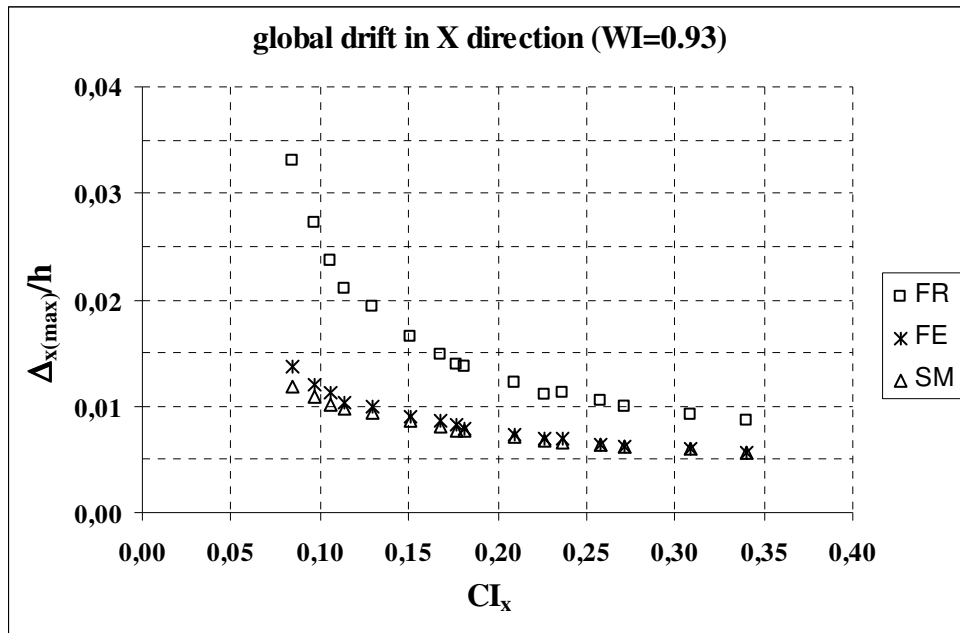


Figure 4.1a - Drift Ratio in X-dir. vs. CI_x for Case I

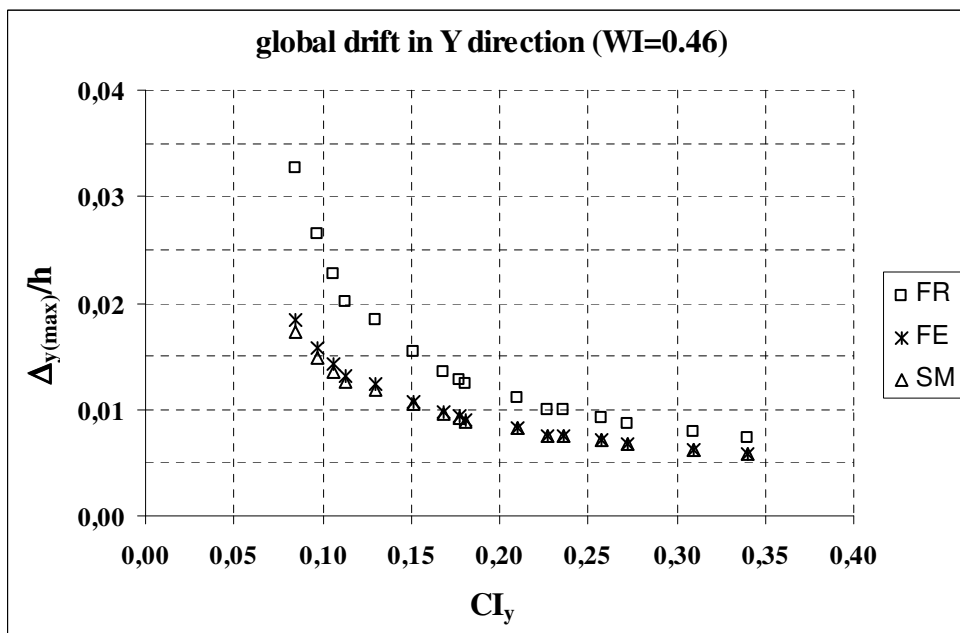


Figure 4.1b - Drift Ratio in Y-dir. vs. CI_y for Case I

The global drift ratio profiles for Case I building can be observed from Figure 4.1a and Figure 4.1b. The effect of column index on the seismic behavior can easily be observed from the results of *FR* model. For $CI = 0.085$, the global drift ratios are 0.0331 in x-direction and 0.0327 in y-direction. As the column indexes increase the global drift ratios decrease. The global drift ratios are 0.0086 in x-direction and 0.0073 in y-direction for $CI = 0.340$. In other words, the global drift ratios for $CI = 0.340$ in both direction are approximately four times smaller than that for $CI = 0.085$. However, the change is nonlinear. The rate of decrease in this range is not constant. For example, in x-direction, total decrease in the global drift ratio is 0.0245 in the range of 0.085-0.340 for CI . 85 % of this reduction takes place up to the mean value of the range ($CI = 0.213$) of column index, remaining 15% takes place in the second half. On the other hand, when the masonry infill walls are included the global drift ratios decrease for all column indexes. This decrease can be explained with the increase of total effective shear area. For $CI = 0.085$, *FR* has approximately 1.65 m^2 of column area resisting lateral forces in x-direction. For this configuration, the global drift ratio is 0.0331. When approximately 17.65 m^2 of masonry infill wall area are added to resist lateral forces, the global drift ratio becomes 0.0137 for *FE* and 0.0118 for *SM*. Additional resistance of masonry infill wall results in the global drift ratios that are 2.4 times less for *FE* and 2.8 times less for *SM*. However, for $CI = 0.340$, when the same amount of masonry infill wall is added to resist lateral forces, the global drift ratios decrease from 0.0086 to 0.0056 (1.5 times) for both *FE* and *SM* in x-direction. The same relation is valid in y-direction. However the additional resistance of masonry infill wall in y-direction is less than that in x-direction because constant wall index is equal to 0.46 while it is equal to 0.93 in x-direction.

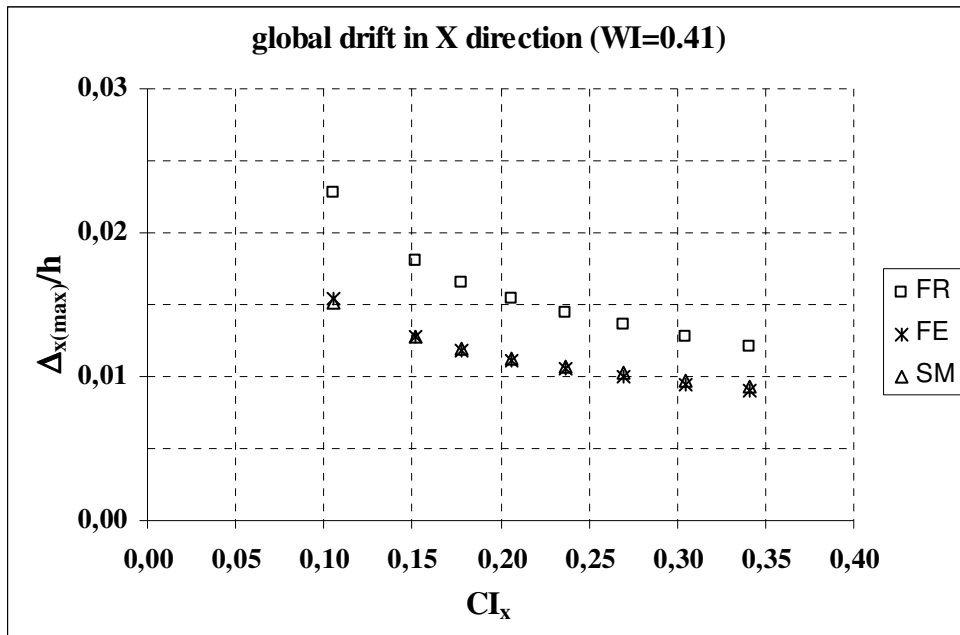


Figure 4.2a - Drift Ratio in X-dir. vs. Cl_x for Case II

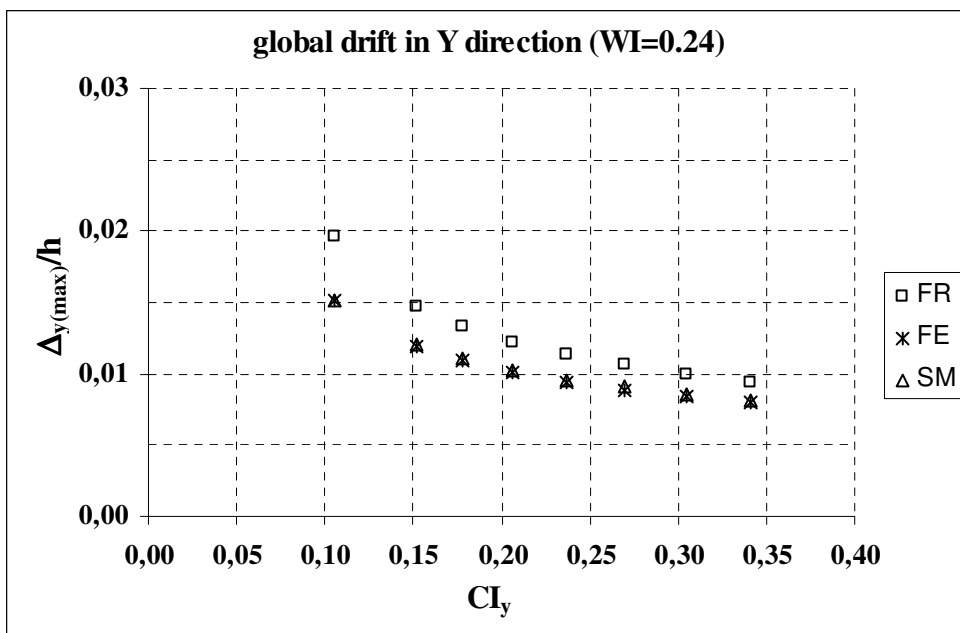


Figure 4.2b - Drift Ratio in Y-dir. vs. Cl_y for Case II

The global drift ratio profiles for Case II can be observed from Figure 4.2a and Figure 4.2b. The results of Case II are similar to the result of Case I. Whether the model consists of masonry infill wall or not, the global drift ratios decrease as column indexes increase. As in Case I, the global drift ratios for masonry infilled frame condition are less than that for bare frame condition. However, the decrease is not constant for all column index values. The contribution of the masonry infill wall decreases as the column index increases. The reduction in the global drift is also presented for both cases in Table 4.3 and Table 4.4.

Table 4.3 - Percentage Reduction in Global Drift Ratio for Case I

BUILDING ID	WI = 0.93			BUILDING ID	WI = 0.46		
	CI_x	(%)Reduction in $\Delta_{x(max)}/h$			CI_y	(%)Reduction in $\Delta_{y(max)}/h$	
		$(1 - \frac{FE}{FR}) * 100$	$(1 - \frac{SM}{FR}) * 100$			$(1 - \frac{FE}{FR}) * 100$	$(1 - \frac{SM}{FR}) * 100$
B2	0,085	58,46	64,23	B2	0,085	43,57	47,31
B5	0,097	55,70	60,01	B10	0,097	40,58	43,99
B6	0,106	52,32	56,72	B18	0,106	37,07	40,39
B7	0,113	51,29	54,16	B30	0,113	34,43	37,65
B10	0,130	48,87	51,72	B5	0,130	32,48	35,62
B12	0,151	45,40	48,25	B12	0,151	30,57	32,03
B14	0,168	41,44	45,81	B19	0,168	28,17	29,55
B15	0,181	42,61	43,98	B6	0,177	27,00	28,37
B18	0,177	41,31	44,10	B31	0,181	26,39	27,72
B19	0,210	40,15	41,49	B14	0,210	24,48	25,76
B21	0,236	38,32	40,91	B7	0,227	24,08	24,10
B27	0,258	38,24	38,24	B21	0,236	23,97	23,98
B30	0,227	37,99	39,30	B32	0,258	22,65	22,65
B31	0,272	37,16	37,16	B15	0,272	22,05	22,06
B32	0,309	35,60	35,60	B27	0,309	20,64	20,64
B33	0,340	34,38	34,38	B33	0,340	20,57	19,57

In Table 4.3 it is seen that for $CI_x = CI_y = 0.085$, the reduction in the global drift ratio is 58% for $WI = 0.93$ while it is only 43% for $WI = 0.46$ by using FEMA 273 [7]. On the other hand, for the same column indexes, if one uses Smith and Carter [6] Method, the reduction in the global drift ratio is 64% for $WI = 0.93$ and it is 47% for $WI = 0.46$. For both FEMA 273 [7] and Smith and Carter [6] Methods reduction in drift ratios decreases as the column indexes increase while keeping wall index constant. It is also seen that reduction in the global drift ratios is greater in *SM* than in *FE* for smaller column indexes. However, as the column indexes increase the differences decrease and become equal after a certain value.

Table 4.4 - Percentage Reduction in Global Drift Ratio for Case II

BUILDING ID	WI = 0.41			BUILDING ID	WI = 0.24		
	CI_x	(%)Reduction in $\Delta_{x(max)}/h$			CI_y	(%)Reduction in $\Delta_{y(max)}/h$	
		$(1 - \frac{FE}{FR}) * 100$	$(1 - \frac{SM}{FR}) * 100$			$(1 - \frac{FE}{FR}) * 100$	$(1 - \frac{SM}{FR}) * 100$
B54	0,105	32,27	33,47	B54	0,105	22,63	22,64
B59	0,152	29,24	29,24	B59	0,152	19,62	18,65
B62	0,178	28,92	27,86	B62	0,178	18,30	17,37
B68	0,207	27,78	26,75	B68	0,207	17,24	16,36
B70	0,237	26,80	25,80	B70	0,237	17,18	15,51
B74	0,270	26,90	24,94	B74	0,270	16,40	14,78
B77	0,305	26,08	24,16	B77	0,305	15,69	14,13
B80	0,341	25,30	23,42	B80	0,341	15,04	13,54

In Table 4.4 it is seen that for $CI_x = CI_y = 0.341$, the reduction in the global drift ratio is 25% for $WI = 0.41$ while it is only 15% for $WI = 0.24$ by using FEMA 273 [7]. On the other hand, for the same column indexes, if one uses Smith and Carter [6] Method, the reduction in the global drift ratio is 23% for $WI = 0.41$ and it is 13% for $WI = 0.24$. For both FEMA 273 [7] and Smith and Carter [6]

Methods, the reduction in drift ratios decreases as the column indexes increase while keeping wall index constant. It is also seen that unlike Case I (Table 4.3), the reduction in the global drift ratios are greater in *FE* than in *SM* for all column indexes. Since the number of stories and the floor areas are different for two case buildings, the column sizes in Case I are smaller than those in Case II for the same *CI* value. For smaller column sizes, the equivalent strut widths obtained from Smith and Carter [6] are greater than those obtained from FEMA 273 [7]. On the other hand, the equivalent strut widths obtained from Smith and Carter [6] are smaller than those obtained from FEMA 273 [7] for greater column sizes.

As inferred from Table 4.3 and Table 4.4, the reduction in global drift ratio decreases while the column index increases. However the range of the reduction is different for each wall index. Also the rate of reduction depends on the range of column index. To visualize these differences, all reduction profiles for each direction in each case are given on the same graph for different wall indexes. (Figure 4.3)

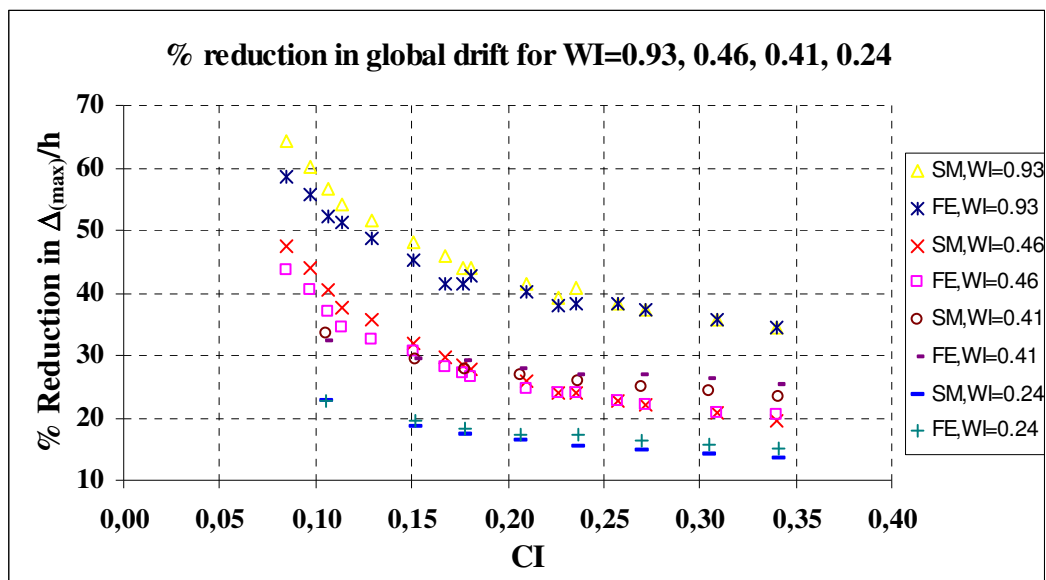


Figure 4.3 – % Reduction in Global Drift Ratio for Different *WI*

In Figure 4.3, as the column size increases, the reduction in global drift decreases. This can be related with the decrease in effectiveness of masonry infill wall with respect to total effective shear area. In other words, as the column size increases, total effective shear area also increases. Since wall area is constant, the share of infill wall in the total effective shear area decreases. Although the reduction range is different for each wall index, all curves tend to converge to a certain value. In other words, the rate of decrease in reduction of global drift ratio becomes smaller with an increase of column index. It is seen that, the range of 0.20 – 0.25 is a critical range for column index. Beyond that range, the change in reduction in global drift ratio becomes almost insignificant. It can be said that, although the effect of masonry infill wall on seismic performance is related with the wall index it is very small when the column index is greater than 0.25.

4.3 EFFECT OF INFILL WALL THICKNESS

To investigate the effect of masonry infill wall at different wall thicknesses, case study buildings were subjected to lateral forces keeping the column sizes constant. Due to number of stories and gravity load requirements, selected column sizes are different for Case I and Case II. Constant column sizes are 50 cm by 50 cm ($CI = 0.236$) for Case I and 65cm by 65cm ($CI = 0.178$) for Case II. The same procedure was followed for both cases and the wall thickness was increased from 20 cm to 35 cm. However, the same infill wall thickness corresponds to different wall indexes because of differences in plan layout between two case buildings. Corresponding wall indexes for the two case study buildings in both x- and y- directions are tabulated in Table 4.5.

Table 4.5 – Wall Index for Different Wall Thicknesses

Wall Thickness (cm)	CASE I			CASE II		
	Building ID	WI_x	WI_y	Building ID	WI_x	WI_y
20	B21	0,93	0,46	B62	0,41	0,24
25	B22	1,16	0,58	B63	0,52	0,30
30	B23	1,39	0,70	B64	0,62	0,35
35	B24	1,62	0,81	B66	0,72	0,41

The global drift ratios of Case I and Case II are given in Table 4.6 and Table 4.7 respectively. It is important to note that all three models (*FR*, *FE* and *SM*) have varying results with the increase of the column sizes, as the column is common structural element for all models. However *FR* model does not contain any wall element. Therefore, any change in wall thickness has no effect on *FR* model. This means that, the global drift ratio obtained from *FR* model is constant for all analyses in this part.

Table 4.6 - Global Drift Ratio for Case I

$CI = 0.236$								
Building ID.	WI_x	WI_y	$\Delta_{x(max)}/h$			$\Delta_{y(max)}/h$		
			<i>FR</i>	<i>FE</i>	<i>SM</i>	<i>FR</i>	<i>FE</i>	<i>SM</i>
B21	0,93	0,46	0,0112	0,0069	0,0066	0,0099	0,0075	0,0075
B22	1,16	0,58		0,0063	0,0062		0,0071	0,0071
B23	1,39	0,70		0,0058	0,0057		0,0069	0,0067
B24	1,62	0,81		0,0056	0,0053		0,0066	0,0064

Table 4.7 - Global Drift Ratio for Case II

$CI = 0.178$								
Building ID.	WI_x	WI_y	$\Delta_{x(max)}/h$			$\Delta_{y(max)}/h$		
			<i>FR</i>	<i>FE</i>	<i>SM</i>	<i>FR</i>	<i>FE</i>	<i>SM</i>
B62	0,41	0,24	0,0166	0,0118	0,0120	0,0133	0,0109	0,0110
B63	0,52	0,30		0,0112	0,0112		0,0104	0,0106
B64	0,62	0,35		0,0106	0,0106		0,0100	0,0102
B66	0,72	0,41		0,0100	0,0100		0,0098	0,0098

By using the results presented in Table 4.6 and Table 4.7, the values of global drift ratio obtained from *FR*, *FE* and *SM* versus wall index are drawn on the same graph for each case, to visualize the difference between the infilled frame (*FE* and *SM*) condition and bare frame (*FR*) condition easily. The results in x and y directions are given in Figure 4.4a and Figure 4.4b, respectively for Case I, and those for Case II are given in Figure 4.5a and Figure 4.5 b.

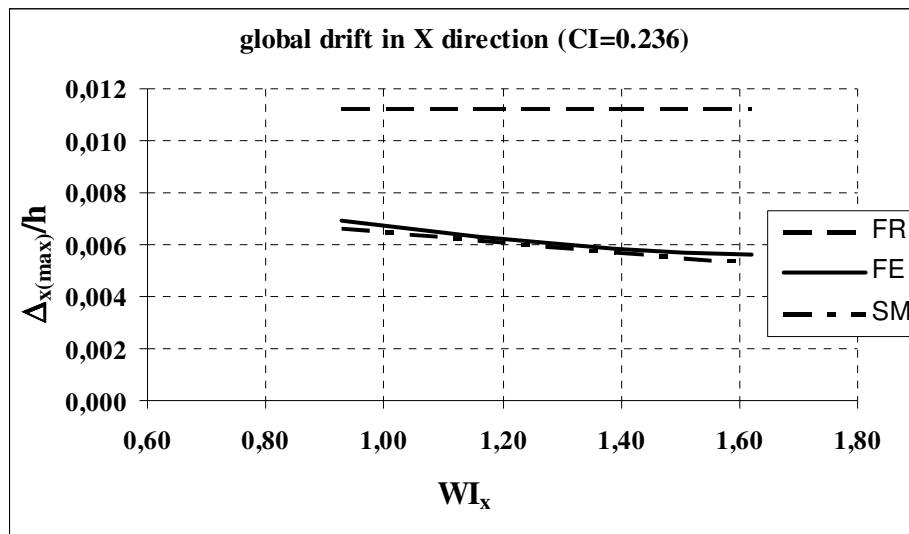


Figure 4.4a - Drift Ratio in X-dir. vs. WI_x for Case I

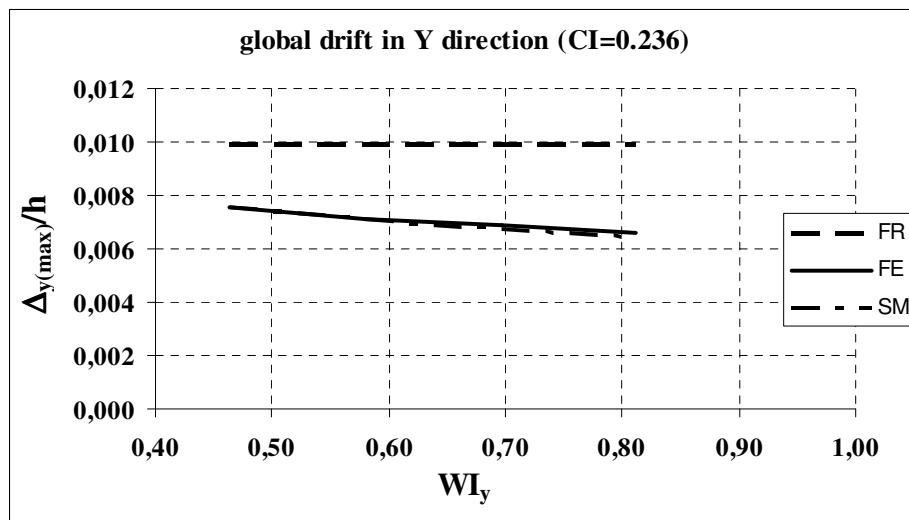


Figure 4.4b - Drift Ratio in Y-dir. vs. WI_y for Case I

In Figure 4.4a and Figure 4.4b, it is seen that for $CI_x = CI_y = 0.236$, the global drift ratios are 0.0112 and 0.0099 for x and y directions respectively for *FR*. Although the column indexes are same in both directions, the difference between frame properties (number of frames and frame bay widths) may cause difference between the global drift ratios. For both *FE* and *SM*, the global drift ratios decrease as the wall indexes increase while the global drift ratios for *FR* are constant. It is also seen that the difference between the global drift ratios of *FE* and *SM* is negligibly. In x-direction, maximum difference is 4% while it is %3 in y-direction. The main difference between two directions is the range of wall index. While the range is between 0.46 and 0.81 in y-direction, it is between 0.93 and 1.62 in x-direction. Therefore, it is expected that the effect of masonry infill wall in x-direction is greater than that in y-direction. Although the global drift ratio in x- direction is greater than the ratio in y-direction for bare frame condition, the global drift ratio is between 0.0069 and 0.0056 for *FE* in x- direction, while it is between 0.0075 and 0.0066 for *FE* in y-direction.

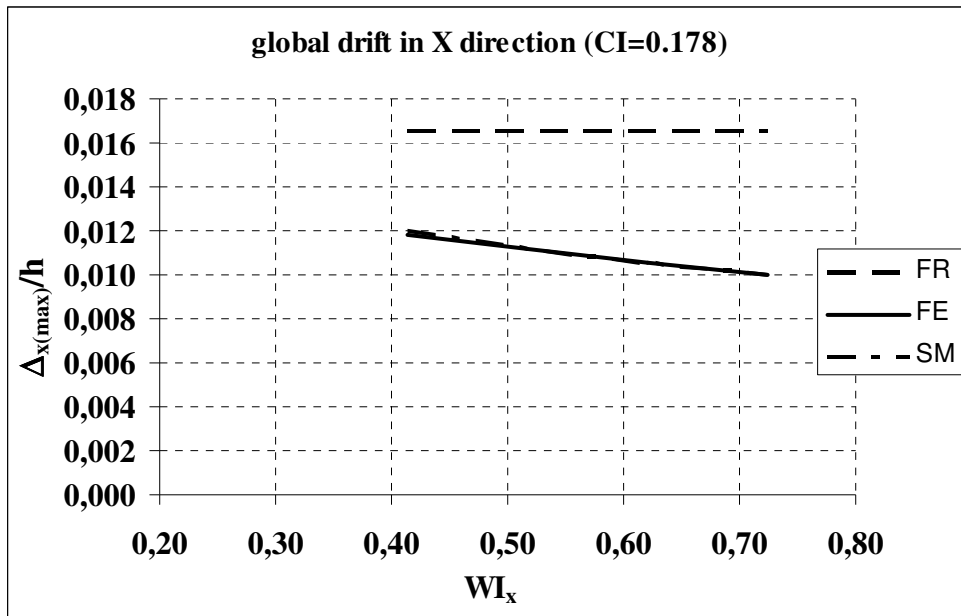


Figure 4.5a - Drift Ratio in X-dir. vs. WI_x for Case II

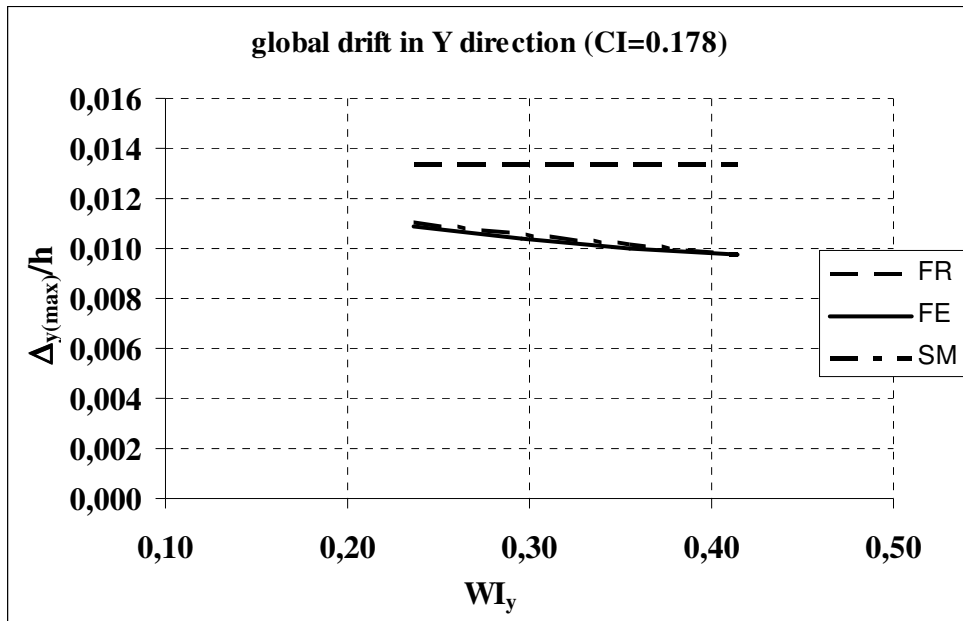


Figure 4.5b - Drift Ratio in Y-dir. vs. WI_y for Case II

In Figure 4.5a and Figure 4.5b, it is seen that for $CI_x = CI_y = 0.178$, the global drift ratios are 0.0166 and 0.0133 for x and y directions respectively for *FR*. Although the column indexes are same in both directions, the difference between frame properties (number of frames and frame bay widths) may cause difference between the global drift ratios. As in Case I, For both *FE* and *SM*, the global drift ratios decrease as the wall indexes increase while the global drift ratios for *FR* are constant. It is also seen that the difference between the global drift ratios of *FE* and that of *SM* is negligibly small. In x-direction, maximum difference is 1% while it is %2 in y-direction. As in Case I, the effect of masonry infill wall in x-direction is greater than that in y-direction, since the same wall thickness is corresponding to grater wall index. For 35 cm thickness of wall, the global drift ratios by using FEMA are almost same in both directions (0.0100 in x-direction and 0.0098 in y-direction), the reduction between *FR* and *FE* is 40% in x-direction, while it is only 26% in y-direction. The greater value of wall index results in greater value of reduction in global drift ratio. To make same

comparison for all wall index values, percentage reduction values in global drift ratio are obtained for both cases and are given in Table 4.8.

Table 4.8 - Percentage Reduction in Global Drift Ratio for Different CI

$CI = 0.236$				$CI = 0.178$			
Building ID.	WI	(%)Reduction in $\Delta_{(max)}/h$		Building ID.	WI	(%)Reduction in $\Delta_{(max)}/h$	
		$(1 - \frac{FE}{FR}) * 100$	$(1 - \frac{SM}{FR}) * 100$			$(1 - \frac{FE}{FR}) * 100$	$(1 - \frac{SM}{FR}) * 100$
B21	0,46	23,97	23,98	B62	0,24	18,30	17,37
B22	0,58	28,17	28,18	B63	0,30	21,78	20,74
B23	0,70	30,47	31,91	B64	0,35	24,96	23,81
B24	0,81	33,72	35,24	B66	0,41	26,63	26,63
B21	0,93	38,32	40,91	B62	0,41	28,92	27,86
B22	1,16	43,57	44,93	B63	0,52	32,36	32,36
B23	1,39	47,95	49,32	B64	0,62	36,27	36,27
B24	1,62	50,20	53,03	B66	0,72	39,70	39,70

It is important to note that for $CI = 0.236$, while the interval of 0.46-0.81 belongs to x-direction, the interval of 0.93-1.62 for wall index belongs to y-direction. Table 4.8 shows that the values of reduction in global drift ratio give complementary result. The reduction in global drift ratio has reasonable increase with the increase of wall index. This increase seems to be independent of direction. Same conclusion can be made for $CI = 0.178$ (Case II). It is also seen that the reduction in global drift ratios are greater in SM than in FE for $CI = 0.236$ (Column sizes: 50cm by 50 cm). However, they are smaller in SM than in FE or they are equal to each other for $CI = 0.178$ (Column sizes: 65cm by 65 cm). As concluded from Table 4.3 and Table 4.4, the reduction in drift ratios are greater in SM than in FE for smaller column sizes. Then, as the column sizes increase this difference decreases and become insignificant. It is also seen that this conclusion is valid for different wall indexes according to Table 4.8.

The reduction profiles for different column indexes are also plotted on the same graph (Figure 4.6)

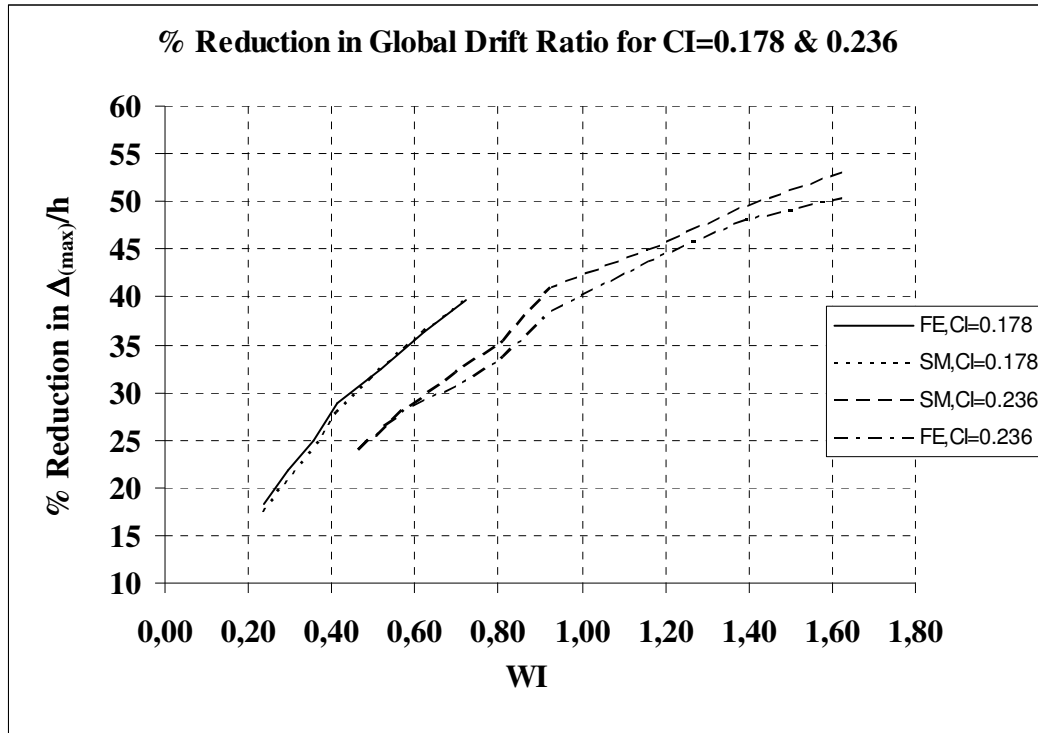


Figure 4.6 – % Reduction in Global Drift Ratio for Different *CI*

According to Figure 4.6, as the infill wall thickness increases, the effect of infill wall on behavior also increases. The reduction values for $CI = 0.178$ are greater than the values for $CI = 0.236$ for the same wall index level. For example; for $WI = 0.60$, the reduction in global drift ratio is approximately 37% for $CI = 0.178$ by using *FE* whereas it is approximately 28% for $CI = 0.236$. This result can be related with the share of infill wall in total effective shear area. In other words, as the column index decreases, the effect of masonry infill wall on the seismic performance of building becomes more significant. According to Figure 4.6, it is also seen that the reduction versus wall index relation is not linear. The rate of increase in reduction is decreasing with the increase of wall index. As

explained in Chapter II, stiffer frame gives better result in behavior of infilled frame and equivalent strut analogy. The equivalent width of masonry infill wall decreases because the relative stiffness of column decreases while wall index increases

4.4 RECOMMENDED RELATION FOR GIVEN GLOBAL DRIFT RATIO

A trial-error process is performed on two case buildings to get recommended relation for column ratio and wall ratio. The column ratio, P_c , is the ratio of the sum of column areas at one story to the floor area of that story and the wall ratio, P_w , is the ratio of the effective wall area in a given direction to the floor area. To initiate the analysis process, different global drift ratios are selected for each building according to their plan layout and their number of stories. The selected global drift ratios are given in Table 4.9.

Table 4.9 – Target Global Drift Ratios

CASE	TARGET GLOBAL DRIFT RATIO		
I	0.003	0.005	0.010
II	0.006	0.010	0.015

To obtain the target global drift ratio, the configurations for column size and wall thickness are determined by trial and error process. The necessary column sizes and wall thicknesses for *FE* are given for each target global drift ratio separately in Tables 4.10 – 4.12 for Case I.

Table 4.10 - Wall-Column Relation for $\Delta_{max} / H = 0.003$ (Case I)

Building ID.	column size (cm)		wall thickness (cm)	P_c	P_w
	b_x	b_y			
B26	50	50	100	0,0071	0,1390
B29	55	55	95	0,0086	0,1321
B35	60	60	84	0,0102	0,1168
B37	65	65	72	0,0120	0,1001
B39	70	70	63	0,0139	0,0876
B41	75	75	54	0,0159	0,0751
B43	80	80	44	0,0181	0,0612
B44	85	85	35	0,0205	0,0487
B45	90	90	26	0,0230	0,0361

Table 4.11 - Wall-Column Relation for $\Delta_{max} / H = 0.005$ (Case I)

Building ID.	column size (cm)		wall thickness (cm)	P_c	P_w
	b_x	b_y			
B1	25	25	122	0,0018	0,1696
B4	30	30	97	0,0026	0,1349
B8	35	35	79	0,0035	0,1098
B13	40	40	64	0,0045	0,0890
B17	45	45	52	0,0057	0,0723
B25	50	50	42	0,0071	0,0584
B28	55	55	35	0,0086	0,0487
B34	60	60	26	0,0102	0,0361
B36	65	65	21	0,0120	0,0292
B38	70	70	15	0,0139	0,0209
B40	75	75	9	0,0159	0,0125
B42	80	80	4	0,0181	0,0056

Table 4.12 - Wall-Column Relation for $\Delta_{max} / H = 0.010$ (Case I)

Building ID.	column size (cm)		wall thickness (cm)	P_c	P_w
	b_x	b_y			
B3	30	30	32	0,0026	0,0445
B9	35	35	22	0,0035	0,0306
B11	40	40	14	0,0045	0,0195
B16	45	45	8	0,0057	0,0111
B20	50	50	1	0,0071	0,0014

Using the results given in Tables 4.10 – 4.12, the recommended relations for three story building are plotted in Figure 4.7.

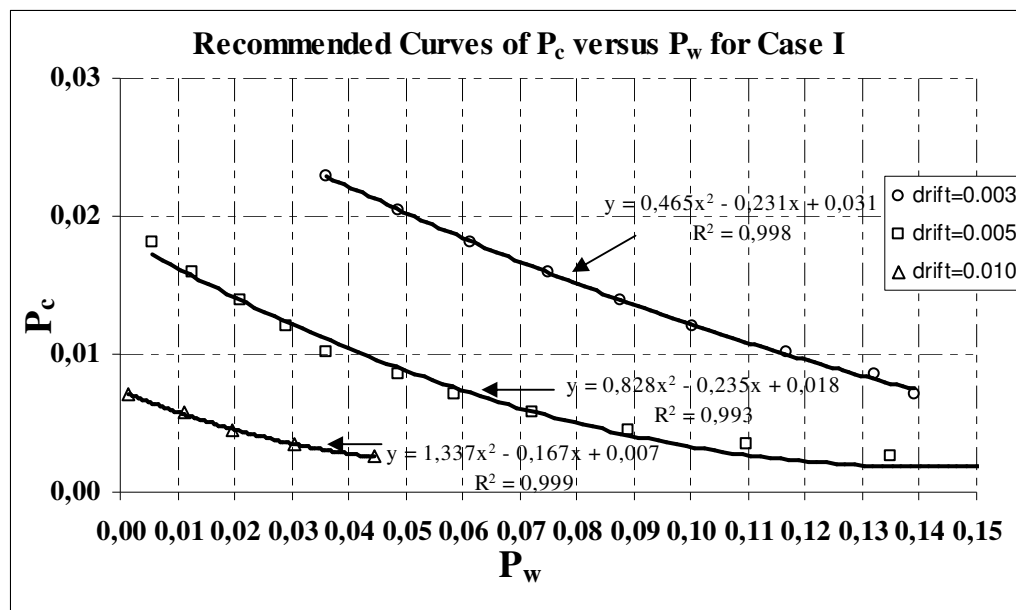


Figure 4.7 - Graph of column ratio versus wall ratio (Case I)

In Figure 4.7, to obtain the algebraic equation for each global drift ratio, the trendlines are assigned to the series. It is seen that the relations obtained by using the results given in Tables 4.10-4.12 are not linear. The column ratio versus the wall ratio relations are second order polynomial with $R^2 \geq 0.99$. It is also seen that the decrease in the column ratio can only be tolerated with much more increase in the wall ratio to achieve the same global drift ratio. The global drift ratio is equal to 0.005 for $P_c = 0.016$ and $P_w = 0.0125$. To get the same global drift ratio with $P_c = 0.0026$, P_w must be equal to 0.1349. In other words, the reduction of effective column area from 10 m^2 to 1.65 m^2 in loading direction can be tolerated with the increase in wall area in that direction from 8 m^2 to 86 m^2 . For the global drift ratio of 0.010, the meaning of the reduction of column ratio from 0.0071 to 0.0026 is the increase of wall index from 0.0015 to 0.045. In other words, 2.8 m^2 of change in effective column area corresponds to 28 m^2 of change in wall area in that direction.

Similarly, for the target global ratio the necessary column sizes and wall thicknesses given in Tables 4.13 – 4.15 for Case II. Recommended relation for global drift curves for the six story building are given in Figure 4.8

Table 4.13 - Wall-Column Relation for $\Delta_{max} / H = 0.006$ (Case II)

Building ID.	column size (cm)		wall thickness (cm)	P_c	P_w
	b_x	b_y			
B72	75	75	90	0,0142	0,1117
B75	80	80	83	0,0162	0,1030
B78	85	85	75	0,0183	0,0931
B81	90	90	66	0,0205	0,0819
B82	100	100	52	0,0253	0,0645
B83	105	105	46	0,0279	0,0571
B84	110	110	40	0,0306	0,0496

Table 4.14 - Wall-Column Relation for $\Delta_{max} / H = 0.010$ (Case II)

Building ID.	column size (cm)		wall thickness (cm)	P_c	P_w
	b_x	b_y			
B57	55	55	50	0,0077	0,0620
B60	60	60	40	0,0091	0,0496
B65	65	65	34	0,0107	0,0422
B69	70	70	28	0,0124	0,0347
B71	75	75	23	0,0142	0,0285
B73	80	80	19	0,0162	0,0236
B76	85	85	14	0,0183	0,0174
B79	90	90	10	0,0205	0,0124

Table 4.15 - Wall-Column Relation for $\Delta_{max} / H = 0.0150$ (Case II)

Building ID.	column size (cm)		wall thickness (cm)	P_c	P_w
	b_x	b_y			
B57	50	50	21	0,0063	0,0261
B60	55	55	14	0,0077	0,0174
B65	60	60	8	0,0091	0,0099
B69	65	65	4	0,0107	0,0050
B71	70	70	1	0,0124	0,0012

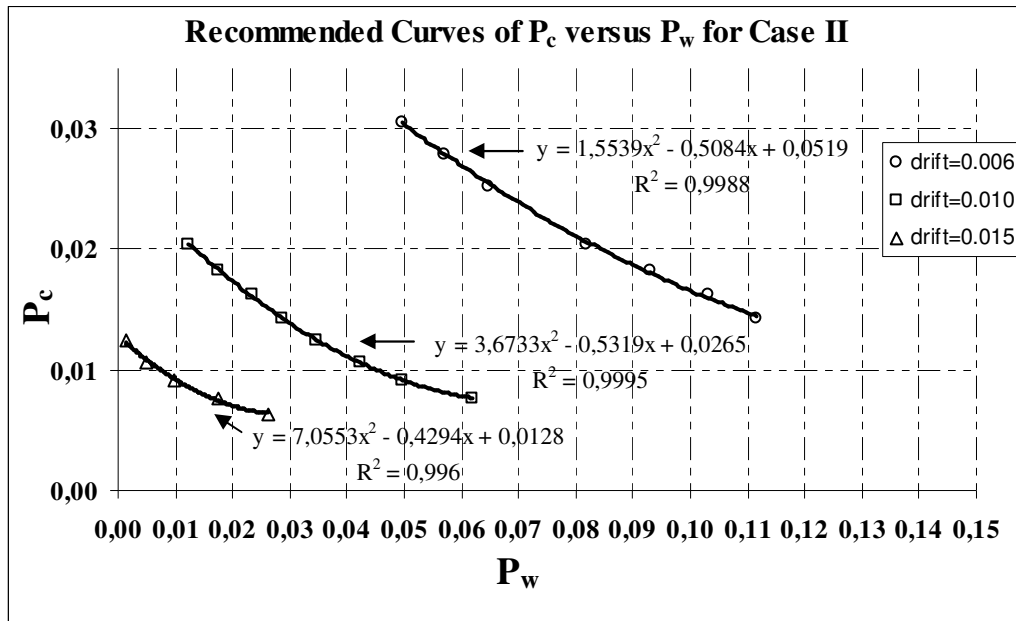


Figure 4.8 - Graph of column ratio versus wall ratio (Case II)

In Figure 4.8, it is seen that the all trendlines are second order polynomial with $R^2 \geq 0.99$. As in Case I, the relations for all global drift ratios are column dominant. The global drift ratio is equal to 0.010 for $P_c = 0.0205$ and $P_w = 0.0124$. To get the same global drift ratio with $P_c = 0.0107$, P_w must be equal to 0.0420. In other words, the reduction of 12 m^2 in effective column area can be tolerated with the increase of 40 m^2 in wall area. Although the curves are not linear, they may be helpful for a designer at the preliminary design stage. The importance of column size and relative infill wall effect can be easily extracted from these helpful curves.

Gülkan and Sözen [14] proposed a similar relation for seismic vulnerability of reinforced concrete frame type buildings consisting of masonry infills. However, their method is simply based on the mean ground story drift, *MGSD*. They indicated that the mean ground story drift, *MGSD*, is directly proportional with the seismic vulnerability of a structure. On the other hand, the relations given in this study are based on the global drift ratio. Therefore, corresponding column

ratio and wall ratio values for the same drift ratio value obtained from this study and Gülkan and Sözen [14] are inconsistent. The column ratio versus the wall ratio relations proposed by Gülkan and Sözen [14] for particular *MGSD* are given in Figure 4.9.

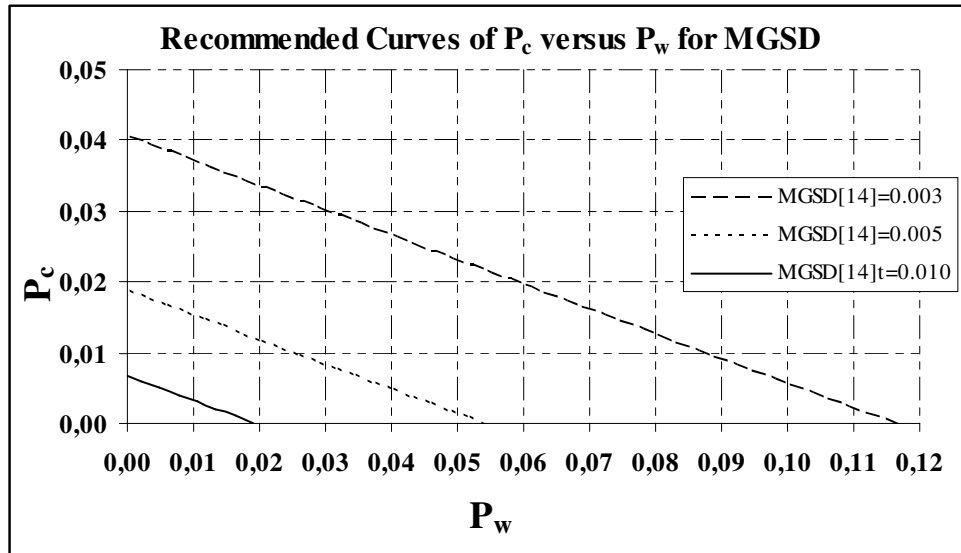


Figure 4.9 – Column and wall ratios required to limit *MGSD*

In Figure 4.9, it is seen that the relations proposed by Gülkan and Sözen [14] for *MGSD* are linear for all mean ground story drift. However the curves in Figure 4.7 and 4.8 are second order polynomial. The difference can be attributed to that other parameters, namely frame geometry, plan layout, number of story etc. may be effective on the seismic behavior.

4.5 EFFECT OF INFILL WALL ARRANGEMENT

To investigate the effect of infill wall arrangement on seismic behavior, three different but symmetric arrangements are used for both cases. The details of the procedure were given in Section 3.3.3.3. In all three models, namely Model I,

Model II and Model III, total wall areas are kept constant by changing the wall thickness.

Analysis results are tabulated in two tables for each case. Results obtained from *FE* and *SM* are listed in Tables 4.16a – 4.17a, respectively for Case I and in Table 4.17a and Table 17.b, respectively for Case II. For both cases, Inter-story drift ratios of Model I are taken as origin and percentage changes relative to Model I are calculated for Model II and Model III.

Table 4.16a - Comparison of Results for *FE* (Case I)

Story	t (cm)	X-direction					Y-direction				
		Model 1		Model 2		Model 3	Model 1		Model 2		Model 3
		$\frac{\Delta_{i_x, max}}{h_i}$ multiplied by 10^{-4}	$\frac{\Delta_{i_x, max}}{h_i}$ multiplied by 10^{-4}	% Change	$\frac{\Delta_{i_x, max}}{h_i}$ multiplied by 10^{-4}	% Change	$\frac{\Delta_{i_y, max}}{h_i}$ multiplied by 10^{-4}	$\frac{\Delta_{i_y, max}}{h_i}$ multiplied by 10^{-4}	% Change	$\frac{\Delta_{i_y, max}}{h_i}$ multiplied by 10^{-4}	% Change
3	20	55,37	55,68	0,56	57,21	3,32	60,88	60,97	0,15	62,27	2,28
	25	49,89	51,74	3,71	51,89	4,01	56,90	58,28	2,43	58,47	2,76
	30	45,42	47,28	4,10	47,83	5,31	54,75	54,90	0,27	55,16	0,75
	35	43,15	43,56	0,95	44,80	3,82	51,74	51,91	0,33	53,63	3,65
2	20	86,20	86,56	0,42	88,50	2,67	93,49	93,58	0,10	95,25	1,88
	25	78,62	81,10	3,15	81,11	3,17	88,17	89,97	2,04	90,17	2,27
	30	72,29	74,83	3,51	75,35	4,23	85,25	85,40	0,18	85,65	0,47
	35	69,03	69,48	0,65	70,96	2,80	81,13	81,29	0,20	83,55	2,98
1	20	66,31	66,50	0,29	67,61	1,96	71,35	71,38	0,04	72,35	1,40
	25	61,69	63,19	2,43	63,12	2,32	68,18	69,24	1,55	69,32	1,67
	30	57,73	59,30	2,72	59,53	3,12	66,42	66,48	0,09	66,59	0,26
	35	55,66	55,91	0,45	56,73	1,92	63,89	63,95	0,09	65,30	2,21

Table 4.16b - Comparison of Results for SM (Case I)

Story	t (cm)	X-direction					Y-direction				
		Model 1		Model 2		Model 3	Model 1		Model 2		Model 3
		$\frac{\Delta_{i_x, max}}{h_i}$ multiplied by 10^{-4}	$\frac{\Delta_{i_x, max}}{h_i}$ multiplied by 10^{-4}	% Change	$\frac{\Delta_{i_x, max}}{h_i}$ multiplied by 10^{-4}	% Change	$\frac{\Delta_{i_y, max}}{h_i}$ multiplied by 10^{-4}	$\frac{\Delta_{i_y, max}}{h_i}$ multiplied by 10^{-4}	% Change	$\frac{\Delta_{i_y, max}}{h_i}$ multiplied by 10^{-4}	% Change
3	20	52,65	54,30	3,13	54,41	3,34	60,86	60,96	0,16	61,12	0,43
	25	48,49	48,86	0,76	49,07	1,20	56,89	57,01	0,21	57,22	0,58
	30	44,03	44,44	0,93	44,75	1,64	53,41	53,57	0,30	53,83	0,79
	35	40,34	40,78	1,09	41,19	2,11	50,35	50,53	0,36	50,85	0,99
2	20	82,45	84,66	2,68	84,64	2,66	93,47	93,57	0,11	93,73	0,28
	25	76,64	77,07	0,56	77,12	0,63	88,16	88,27	0,12	88,48	0,36
	30	70,29	70,75	0,65	70,89	0,85	83,43	83,57	0,17	83,83	0,48
	35	64,94	65,42	0,74	65,65	1,09	79,20	79,37	0,21	79,67	0,59
1	20	64,04	65,35	2,05	65,28	1,94	71,34	71,38	0,06	71,45	0,15
	25	60,47	60,70	0,38	60,64	0,28	68,17	68,22	0,07	68,30	0,19
	30	56,47	56,72	0,44	56,69	0,39	65,31	65,36	0,08	65,47	0,24
	35	53,01	53,28	0,51	53,28	0,51	62,70	62,76	0,10	62,89	0,30

In Tables 4.16a and Table 4.16b, it is inferred that there is no regular change in percentage change as the wall index increases. As an example; for third story in x-direction (*FE*), for $WI = 0.93$, percentage change is 0.56 % between Model I and Model II. When $WI = 1.16$, it becomes equal to 3.71 %. It seems that percentage change increases as the wall index increases while keeping the column index constant. However, it is reduced to 0.95 % for $WI = 1.62$. On the other hand, while going from top story to bottom story, the percentage change decreases for all models in both directions provided that the wall index is constant. In Table 4.16b, it is seen that for $WI = 0.93$, percentage changes between Model I and Model II are 3.13 %, 2.68 % and 2.05 % for story 3, story 2 and story 1, respectively. Similarly, the value between Model I and Model III for the same wall index are 3.34 %, 2.66 % and 1.94 % for story 3, story 2 and story 1 respectively. It is also seen that all percentage change values for *FE* and *SM* are

in the range of 5 %. Thus, such an approximate result shows that if the symmetry is satisfied, arrangement of masonry infill walls has no significance in seismic behavior of symmetric building systems.

For Case II, Inter-story drift ratios of Model 1 are taken as origin and percentage changes relative to Model I are calculated for Model II and Model III. And are tabulated in Table 4.17a for *FE* and in Table 4.17b for *SM*

Table 4.17a - Comparison of Results for *FE* (Case II)

Story	t (cm)	X-direction					Y-direction				
		Model 1		Model 2		Model 3	Model 1		Model 2		Model 3
		$\frac{\Delta_{i, max}}{h_i}$ multiplied by 10^{-4}	$\frac{\Delta_{i, max}}{h_i}$ multiplied by 10^{-4}	% Change	$\frac{\Delta_{i, max}}{h_i}$ multiplied by 10^{-4}	% Change	$\frac{\Delta_{i, max}}{h_i}$ multiplied by 10^{-4}	$\frac{\Delta_{i, max}}{h_i}$ multiplied by 10^{-4}	% Change	$\frac{\Delta_{i, max}}{h_i}$ multiplied by 10^{-4}	% Change
6	20	29,36	30,17	2,76	30,15	2,69	28,65	28,70	0,17	29,18	1,85
	25	27,79	28,17	1,37	28,18	1,40	27,08	27,61	1,96	27,70	2,29
	30	26,04	26,47	1,65	27,06	3,92	25,67	26,25	2,26	26,40	2,84
	35	24,55	25,02	1,91	25,66	4,52	24,95	25,12	0,68	25,82	3,49
5	20	48,75	49,94	2,44	49,87	2,30	45,98	46,04	0,13	46,72	1,61
	25	46,21	46,68	1,02	46,66	0,97	43,73	44,47	1,69	44,59	1,97
	30	43,36	43,89	1,22	44,78	3,27	41,70	42,52	1,97	42,68	2,35
	35	40,90	41,48	1,42	42,44	3,77	40,64	40,75	0,27	41,72	2,66
4	20	66,89	68,43	2,30	68,29	2,09	61,66	61,72	0,10	62,56	1,46
	25	63,42	63,96	0,85	63,85	0,68	58,83	59,74	1,55	59,87	1,77
	30	59,50	60,09	0,99	61,25	2,94	56,26	57,27	1,80	57,45	2,12
	35	56,08	56,72	1,14	57,95	3,33	54,91	55,01	0,18	56,22	2,39
3	20	79,51	81,23	2,16	81,03	1,91	72,34	72,39	0,07	73,31	1,34
	25	75,47	76,02	0,73	75,84	0,49	69,21	70,20	1,43	70,33	1,62
	30	70,88	71,48	0,85	72,78	2,68	66,35	67,45	1,66	67,63	1,93
	35	66,84	67,50	0,99	68,87	3,04	64,83	64,92	0,14	66,25	2,19
2	20	80,95	82,49	1,90	82,29	1,66	73,58	73,62	0,05	74,45	1,18
	25	77,21	77,67	0,60	77,47	0,34	70,75	71,64	1,26	71,76	1,43
	30	72,91	73,42	0,70	74,59	2,30	68,15	69,13	1,44	69,29	1,67
	35	69,09	69,65	0,81	70,89	2,61	66,75	66,81	0,09	68,03	1,92
1	20	48,07	48,78	1,48	48,68	1,27	44,94	44,95	0,02	45,34	0,89
	25	46,33	46,54	0,45	46,43	0,22	43,60	44,01	0,94	44,08	1,10
	30	44,30	44,53	0,52	45,07	1,74	42,36	42,82	1,09	42,90	1,27
	35	42,46	42,72	0,61	43,30	1,98	41,69	41,71	0,05	42,30	1,46

Table 4.17b - Comparison of Results for SM (Case II)

Story	t (cm)	X-direction					Y-direction				
		Model 1		Model 2		Model 3	Model 1		Model 2		Model 3
		$\frac{\Delta_{i_x, max}}{h_i}$ multiplied by 10^{-4}	$\frac{\Delta_{i_x, max}}{h_i}$ multiplied by 10^{-4}	% Change	$\frac{\Delta_{i_x, max}}{h_i}$ multiplied by 10^{-4}	% Change	$\frac{\Delta_{i_y, max}}{h_i}$ multiplied by 10^{-4}	$\frac{\Delta_{i_y, max}}{h_i}$ multiplied by 10^{-4}	% Change	$\frac{\Delta_{i_y, max}}{h_i}$ multiplied by 10^{-4}	% Change
6	20	29,85	30,18	1,11	30,15	1,01	29,07	29,12	0,17	29,18	0,38
	25	27,79	28,17	1,37	28,18	1,40	27,54	27,61	0,25	28,16	2,25
	30	26,04	26,47	1,65	26,54	1,92	26,17	26,25	0,31	26,89	2,75
	35	24,55	25,02	1,91	25,14	2,40	24,95	25,12	0,68	25,83	3,53
5	20	49,54	49,95	0,83	49,87	0,67	46,59	46,64	0,11	46,72	0,28
	25	46,21	46,68	1,02	46,66	0,97	44,40	44,47	0,16	45,26	1,94
	30	43,36	43,89	1,22	43,92	1,29	42,43	42,52	0,21	43,40	2,29
	35	40,90	41,48	1,42	41,56	1,61	40,64	40,75	0,27	41,71	2,63
4	20	67,97	68,43	0,68	68,29	0,47	62,41	62,46	0,08	62,56	0,24
	25	63,42	63,96	0,85	63,85	0,68	59,67	59,74	0,12	60,72	1,76
	30	59,49	60,09	1,01	60,03	0,91	57,18	57,27	0,16	58,36	2,06
	35	56,08	56,72	1,14	56,71	1,12	54,91	55,01	0,18	56,20	2,35
3	20	80,75	81,23	0,59	81,03	0,35	73,17	73,20	0,04	73,31	0,19
	25	75,47	76,02	0,73	75,84	0,49	70,15	70,20	0,07	71,28	1,61
	30	70,87	71,48	0,86	71,34	0,66	67,38	67,45	0,10	68,66	1,90
	35	66,84	67,50	0,99	67,39	0,82	64,83	64,92	0,14	66,24	2,17
2	20	82,09	82,49	0,49	82,29	0,24	74,33	74,35	0,03	74,45	0,16
	25	77,20	77,67	0,61	77,47	0,35	71,61	71,64	0,04	72,62	1,41
	30	72,91	73,42	0,70	73,23	0,44	69,09	69,13	0,06	70,23	1,65
	35	69,09	69,65	0,81	69,48	0,56	66,75	66,81	0,09	68,02	1,90
1	20	48,60	48,78	0,37	48,68	0,16	45,28	45,29	0,02	45,34	0,13
	25	46,33	46,54	0,45	46,43	0,22	44,01	44,01	0,00	44,48	1,07
	30	44,29	44,53	0,54	44,42	0,29	42,81	42,82	0,02	43,35	1,26
	35	42,46	42,72	0,61	42,61	0,35	41,69	41,71	0,05	42,29	1,44

In Table 4.17a and 4.17b, it is seen that the disorder in the percentage change takes place as the wall index increases. On the other hand, while going from the sixth story to first story, the percentage change decreases for all models in both directions provided that the wall index is constant. In Table 4.17a, it is seen that for $WI = 0.41$, percentage changes between Model I and Model II are 2.76 %, 2.44 %, 2.30 %, 2.16 %, 1.90 % and 1.48 % from top to bottom, respectively. Similarly, the value between Model I and Model III for the same wall index are

1.85 %, 1.61 %, 1.46 %, 1.34 %, 1.18 % and 0.89 % in the same order. It is also seen that all percentage change values for FE and SM are in the range of 3.5%. Thus, such an approximate result shows that if the symmetry is satisfied, arrangement of masonry infill walls has no significance in seismic behavior of symmetric building systems. Moreover this result is also related with the significance of infill walls in total effective shear area. For Case I masonry infill walls have more effectiveness in total shear area than those in Case II. This situation Results in 5 % of maximum change in Case I, while maximum change is about 3.5 % in Case II.

CHAPTER 5

CONCLUSIONS AND RECOMMENDATIONS

5.1 INTRODUCTION

The main objective of this study was to investigate the effect of hollow masonry infill wall on the seismic performance of R/C buildings. In order to include the hollow masonry infill walls into the analyses model two different approaches were used: namely Smith and Carter method [6] and FEMA 273 method [7]. According to these two approaches, hollow masonry infill walls were modeled as diagonal compression struts. In order to compare and understand the effect of hollow masonry infill walls, analyses were also carried out for bare frames, i.e. without any non-structural infill walls. All analyses were performed on the selected case buildings. These buildings had symmetric plan layout and also had symmetric infill wall arrangement. The difference between them was that Case I building had three stories while Case II had six. Also plan dimensions were different from each other. Several analyses were performed on these two case buildings. The analyses were performed phase by phase to explore the effect of different parameter on behavior. These parameters are column size, infill wall thickness and arrangement of infill walls.

5.2 CONCLUSIONS

Under the light of the results of this analytical study, following conclusions can be drawn;

- The effect of hollow masonry infill walls on the seismic performance of buildings is not constant for different column index. The effect decreases as the column index increases. For flexible frame condition, i.e. smaller value of column index, masonry infill walls have significant effect on the behavior. The reduction in global drift ratio can be as much as 60 percent depending on wall index. On the other hand, for larger column index, this reduction is reduced to 15 percent. If the column index is greater than 0.25, the effect of the hollow masonry infill walls on the behavior of the buildings which have symmetric floor plan and wall arrangements is not significant.
- While keeping the column index constant, increase in wall index causes increase in the contribution of masonry infill wall on the behavior. However, as the wall index increases, the relative stiffness of frame with respect to infill wall decreases. This decrease also causes reduction in the effect of masonry infill wall for greater wall index.
- The seismic behavior of reinforced concrete buildings is dominated by columns. The column is a primary element of lateral load resisting system. The decrease in column index can only be tolerated with much more increase in wall index to achieve same global drift ratio. Although Gülkan and Sözen [14] indicated a linear relationship between the column ratio and the wall ratio, the relationship between the column ratio and the wall ratio to limit the global drift ratio were observed to be nonlinear (parabolic). The additional effects of plan layout, frame geometry are believed to cause this difference.

- Distribution of the masonry infill walls throughout the story has insignificant effect on seismic behavior of reinforced concrete buildings provided that symmetric plan layout of a building and symmetric arrangement of the infill walls are satisfied. The results show that the differences in the global drift ratios for three different symmetric wall arrangements are within 5 %.
- When two approaches which were used for inclusion of hollow masonry infill walls as a diagonal compression strut are compared, it is seen that the global drift ratios obtained from the *SM* model and the *FE* model are close to each other. Although the results were close to each other, it can be said that Smith and Carter [6] gives greater equivalent strut widths than FEMA 273 [7] for smaller column sizes. As the column sizes increase the differences between the equivalent strut widths decrease and become equal after a certain value. However, equivalent strut widths obtained from FEMA 273 [7] become greater than the values obtained from [6] with the further increase in column sizes.

5.3 RECOMMENDATIONS

The following are recommended for the future studies;

- The same study should be carried out on asymmetric buildings.
- To generalize the findings of this study, other building plans and layouts might be employed.
- In order to investigate the effect of the masonry infill walls in inelastic range, non-linear analyses should be performed on same buildings.

REFERENCES

1. T.C. Bayındırlık ve İskan Bakanlığı, “Afet Bölgelerinde Yapılacak Yapılar Hakkında Yönetmelik” (ABYYHY-98), Türkiye Hazır Beton Birliği, 1999.
2. Sucuoğlu, H. and McNiven, H. D. “Seismic Shear Capacity of Reinforced Masonry Piers”, *Journal of Structural Engineering*, Vol. 117, No. 7, pp. 2166-2187, July 1991.
3. Sucuoğlu, H. and Erberik, A., “Performance Evaluation of a Three-Storey Unreinforced Masonry Building During the 1992 Erzincan Earthquake”, *Earthquake Engineering and Structural Dynamics*, Vol. 26, pp. 319-336, 1997.
4. Paulay, T. and Priestley, M. J. N, *Seismic Design of Reinforced Concrete and Masonry Buildings*”, John Wiley & Sons, Inc., 1992.
5. Smith, B. S. and Coull, A., “Tall Building Structures: Analysis and Design”, John Wiley & Sons, Inc., 1991.
6. Smith, B.S. and Carter, C., “A Method of Analysis for Infilled Frames”, *Proc. ICE*, Vol. 44, pp.31-48, September 1969.

7. Applied Technology Council, "NEHRP Guidelines for the Seismic Rehabilitation of Buildings" (ATC 33), Federal Emergency Management Agency Report FEMA 273, Washington 1997.
8. Computer and Structures, Inc., "ETABS Nonlinear Version 8.1.1", California, 2002.
9. Polyakow, "Masonry in framed buildings", Gosudarstvennoe isdatel'stvo Literaturny po stroitel'stvu i arkhitecture, Moscow, 1956.
10. Computer and Structures, Inc., "SAP2000 Nonlinear Version 8.2.3", California, 2003.
11. Ersoy, U., "Reinforced Concrete", Middle East Technical University, Ankara, 2000.
12. Erdem, I., "Strengthening of Existing Reinforced Concrete Frames", M. Sc. Thesis, Middle East Technical University, August 2003.
13. TS-498, "Design Loads for Buildings", Turkish Standards Institute, Ankara, November 1997.
14. Gülkan, P. and Sözen, M.A., "Procedure for Determining Seismic Vulnerability of Building Structures", ACI Structural Journal, Vol. 96, No.3, pp. 336-342, 1999.
15. Ersoy, U. and Marjani, F., "Behavior of Brick Infilled Reinforced Concrete Frames Under Reversed Cyclic Loading", ECAS 2002 International Symposium on Structural and Earthquake Engineering Symposium Proceedings, pp. 142-150, October 2002.

16. Demir, F. and Sivri, M., "Earthquake Response of Masonry Infilled Frames", ECAS 2002 Internatiol Symposium on Structural and Earthquake Engineering Symposium Proceedings, pp. 151-158, October 2002.
17. TS-500,"Requirements for Design and Construction of Reinforced Concrete Structures", Turkish Standards Institute, Ankara, February 2000.